1965

Model study of a folded plate roof

Graham G. Sutherland

T 1809
c. 1

270

MODEL STUDY OF A FOLDED PLATE ROOF

BY

319A

GRAHAM G. SUTHERLAND III, 1942

57p

A

THESIS

submitted to the faculty of the

UNIVERSITY OF MISSOURI AT ROLLA

in partial fulfillment of the requirements for the

Degree of

MASTER OF SCIENCE IN CIVIL ENGINEERING

Rolla, Missouri

1965

Approved by

Joseph V. Senne (advisor) Paul R. Munger

Peter G. Hansen   T. G. Walters

ABSTRACT

The purpose of this study was to conduct a model study of a folded plate roof in order to determine the feasability of using model studies as a method of design. Dimensional analysis was used to derive prediction equations for determining the stresses in two prototype structures, when the stresses in the model were known.

One model and two prototype folded plate roofs were constructed of plexiglas. SR-4 strain gages were attached to the stuctures and strain readings taken as a uniform vertical load was applied in increments. From the strains the stresses at various points in the folded plates were computed.

The analytical, predicted, and experimental stresses were compared for the two prototypes. It was found that the predicted and experimental stress values agreed within 13% at the center of the roof, but near the boundaries of the structure the deviation was much more variable.

ACKNOWLEDGMENT

The author especially wishes to express his thanks to Dr. J. H. Senne for his guidance throughout this research.

The author is grateful to fellow graduate students Leroy Hulsey, Alan Kamp, and Richard Rintoul, for their helpful suggestions and assistance.

Many thanks are also due John Smith for his help in preparing and fabricating the folded plates.

TABLE OF CONTENTS

LIST OF FIGURES

LIST OF TABLES

LIST OF SYMBOLS

A	Area
a	Height of edge plate
b	Constant for SR-4 rosette gage
c	Distance from neutral axis to stress location
C	Coefficient of pi term expression
c_i	Exponent of quantity
d	Width of two plates
E	Young's Modulus
F	Force
h	Height of folded plate
I	Moment of inertia
L	Length
M	Moment
m	Subscript (refers to model parameters)
N	Any point
n	Scale ratio of prototype to model
P	Load
q	Uniform load
R	Apparent strain
s	Length of folded plate
t	Thickness of plate
V	Shear force
x	Longitudinal axis
y	Transverse axis

LIST OF SYMBOLS (Cont.)

δ	Deflection
ϵ	True strain
f	function of
γ	Shearing strain
λ	Any dimension of folded plate
π	Pi term
ϕ	Rotation of principal stress from "x" axis
σ	Normal Stress
μ	Poisson's Ratio

I. INTRODUCTION

The rapid increase in the use of folded plate roofs by architects in recent years has presented the structural engineer with a definite problem in design and analysis. Many analytical approaches have been made, resulting in varied degrees of sucess. The method investigated in this study is the use of a model to design the prototype structure.

The analytical methods formulated to date usually have a number of disadvantages which fall into one or more of the following categories: inaccurate, complex, or nonversatile.

Some of the methods are in error in general, while others may insure an accurate analysis at one location in the structure but not at another. The approach considering the folded plate as a simple beam is not difficult, but its use seldom results in giving the true picture of the stresses in the plate, mainly because it disregards too many factors. On the other hand, the method presented by Born (1) appears to be within engineering accuracy in the central region of the roof, but is in considerable error near the boundaries of the structure.

Most methods employed require considerable time in their solution, either because they are complex in nature or because they involve an iterative process. Several approaches, such as the one based on the minimum energy principle (2), necessitate knowledge above that with which an average graduate civil engineer would be familiar. When the computations, which are sometimes quite rigorous, have been completed, the designer may not be much better off than if he had used the simple beam approach.

The author feels the greatest disadvantage of most analytical methods is their lack of generality or versatility. Some solutions either break down near the supports or must be altered if the plate is anything other than simply supported. Others become difficult or impossible to use if the load is not uniform and symmetrical. One may find a method which works well for a particular folded plate, but does not necessarily work for a plate of a different shape.

The disadvantages of the analytical methods outlined in the previous paragraphs are the main reasons it is felt a model study would be of great assistance in designing folded plates. In reviewing literature it was found that very little work has been done using models, other than a study by Ronald E. Shaeffer (3), and that was for a hyperbolic paraboloid. A large num- of model studies were made only to check an analytical approach, and not to predict a prototype structure.

A model study appears to be the most accurate approach presently available. In addition, savings in materials and design time are possible.

II. DIMENSIONAL ANALYSIS AND SIMILITUDE

A. Introduction

Through the use of dimensional analysis and similitude (4) the author will develop a model of a folded plate roof structure and predict the stress behavior of two prototypes. The shape of the folded plate chosen for this research is shown in Figure 1, and is selected because of its popularity as a roof and for its simplicity of construction. Tests on any other folded plate could be made in a similar manner.

B. Pi terms

Listed below are the variables which are factors in determining the stress at any point in a simply supported folded plate as shown in Figure 1.

Variable	Symbol	Basic dimension
height of edge plate	a	L (length)
height of folded plate	h	L
width of two plates	d	L
length of plate	s	L
thickness of plate	t	L
longitudinal dist. to "N"	x	L
transverse dist. to "N"	y	L
any distance	λ	L
uniform load	q	FL^{-2} (F=force)
distance from neutral axis	c	L

Variable	Symbol	Basic dimension
stress at any point "N"	σ	FL^{-2}

Using these variable two sets of pi terms (dimensionless quantities) were developed. This was necessary to arrive at separate prediction factors for stresses at the transverse center line and ends of the folded plate. It was assumed that all stresses at center span were due to moment only and those at the end were the result of shear only.

For the stresses at mid span it can be said

$$\sigma = f(\, q,\ s,\ c,\ I,\ \lambda\,)$$

or $1 = C_\alpha \sigma^{c_1},\ q^{c_2},\ s^{c_3},\ c^{c_4},\ I^{c_5},\ \lambda^{c_6},$ where C_α is a constant and c_1 through c_6 are exponents of the variables. Putting the variables in terms of their dimensions,

$$0 = C_\alpha (FL^{-2})^{c_1},\ (FL^{-2})^{c_2},\ L^{c_3},\ L^{c_4},\ L^{4c_5},\ L^{c_6}.$$

Equating exponents of "L" on both sides of the equations,

$$0 = -2c_1 - 2c_2 + c_3 * c_4 + 4c_5 + c_6\,,$$

and for "F", $0 = c_1 + c_2$.

Let $c_4 = 1$, $c_2 = c_3 * c_5 = 0$.

Therefore $c_6 = -1$, $c_1 = 0$.

This results in $\pi_1 = \dfrac{c}{\lambda}$.

Similarly, $\pi_2 = \dfrac{I}{\lambda^4}$, $\pi_3 = \dfrac{s}{\lambda}$.

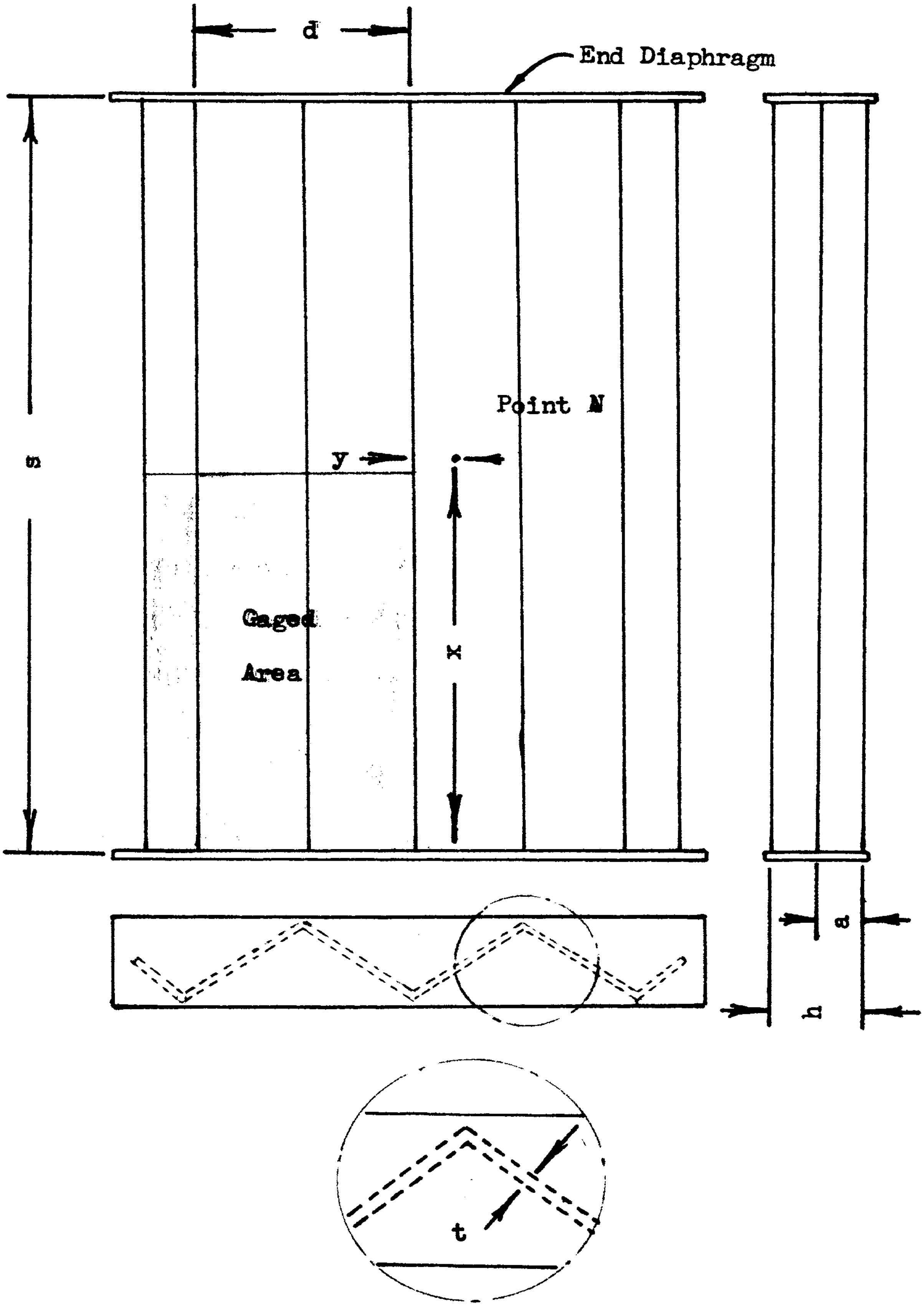

Figure 1. Diagram of folded plate

Next, let c_3 through $c_6 = 0$ and $c_1 = 1$.
Then $-2c_1 - 2c_2 = 0$, and $c_1 + c_2 = 0$.
Solving simultaneously, $c_2 = -1$, and $\pi_4 = \frac{\sigma}{q}$.

Using a similar procedure, the pi terms were developed for the effect of shear by letting $\sigma = f(q, \lambda, t, s)$. Therefore $\pi_1 = \frac{t}{\lambda}$, $\pi_2 = \frac{s}{\lambda}$, $\pi_3 = \frac{\sigma}{q}$.

C. Prediction equations

From elementary mechanics of materials it is known that $\sigma = \frac{Mc}{I}$. Therefore $f(\frac{s}{\lambda}, \frac{I}{\lambda^4}, \frac{c}{\lambda}) = \frac{\lambda s^2 c}{I}$, and for the model $\sigma_m = \frac{\lambda_m s_m^2 c_m}{I_m}$ where the subscript "m" refers to the parameters of the model. Dividing the general equation of the prototype by the general equation of the model,

$$\frac{\frac{\sigma}{q}}{\frac{\sigma_m}{q_m}} = \frac{\frac{\lambda s^2 c}{I}}{\frac{\lambda_m s_m^2 c_m}{I_m}},$$

and reducing,
$$\frac{\sigma}{\sigma_m} = \frac{\lambda s^2 c\ I_m q_m}{\lambda_m s_m^2 c_m I\ q}.$$

If $q = q_m$,
$$\sigma = \frac{\lambda s^2 c\ I_m \sigma_m}{\lambda_m s_m^2 c_m I},$$

which is the prediction equation for stresses at center span. This equation is also used to predict the stresses at the quarter points since moment is the predominant factor there.

It follows that for the prediction equation considering shear only, $\frac{\sigma}{q} = f(\frac{t}{\lambda}, \frac{s}{\lambda})$. From mechanics of materials it is known that $\sigma = \frac{V}{A}$. Therefore

$$\frac{\sigma}{q} = \frac{\lambda s}{\lambda t} = \frac{s}{t}\text{ , the general equation.}$$

Using a procedure similar to that involving moment, the prediction equation for stresses caused by shear becomes

$$\sigma = \frac{s\ t_m \sigma_m}{s_m t}\ ,\quad \text{if } q = q_m.$$

By making use of the above equations and determining the stress at various points in the model, it is a simple matter to predict the stress at corresponding points in the prototype.

D. Model selection

While it is best to retain a geometric similarity between model and prototype, it is sometimes necessary to distort one or more of the dimensions. In a model such as the one in this study the most likely variable that would be necessary to distort is the thickness, since in many cases the model thickness is too small for practical purposes if the model thickness is to scale. At other times, materials are not available that satisfy the scale ratio. The author's reason for distorting the length in one of the prototypes was convenience. It allowed a second prototype to be constucted in which to predict stress.

III. EXPERIMENTATION

A. Materials

The material used for the model and prototypes was an acrylic plastic called plexiglas G. This material was specified to be satisfactory for a model study if the stress did not exceed 1000 p.s.i. (5). The main factor in choosing plexiglas was its good workability qualities during fabrication.

In order to determine the stresses in the plastic from the strains produced, Poisson's Ratio and Young's Modulus were required. Tests to determine these were made as outlined in Appendices 1 and 2.

B. Fabrication

The construction involved cutting the plexiglas to the correct dimensions, fastening the pieces together to form a folded plate, attaching the strain gages, and building the loading tree.

Each folded plate was formed by adhering five pieces of plexiglas using chloroform as an adhesive. Two adjacent strips of plastic were clamped into the desired position and the chloroform injected between the surfaces in contact. The chloroform temporarily dissolved the plexiglas. Upon rehardening, the result was a bond nearly as strong as the material itself. Dimensions of each structure appear in Table I.

The ends of each folded plate were recessed 1/8 inch into a diaphragm made of 3/8 inch plexiglas and firmly glued. This was done to prevent any transverse spreading of the plates at the ends. At the same time, this left the plates free to rotate about a transverse axis at both ends.

The loading system was constructed to enable a uniform load to be closely approximated. It consisted of triangular shaped devices made of 1/4 inch plywood and 1/8 inch diameter bolts (Figure 2). Each triangle transmitted three point loads of the same magnitude to the folded plate as shown in Figure 3. Three-sixteenth inch square rubber pads were glued to the plate's surface under each bolt to help distribute the load and and stabilize the triangles. To transmit the load to the triangles, a monolithic plastic line was attached at the center of gravity of each triangle and passed vertically through a hole in the roof to a loading tree.

The loading tree consisted of several simple beams that reduced each 10 or 20 loads to one. This enabled the folded plate to be loaded with 150 (model and prototype II) or 300 (prototype I) point loads by hanging three or five weights at the base of the loading tree. This loading system is pictured in Figures 4 and 5. The second prototype (II) was loaded in a slightly different

Variable	Dimensions (inches)		
	Model	Prototype I	Prototype II
a	2	2	3
h	4	4	6
s	30	60	45
d	8	8	12
t	1/8	1/8	1/8

Table I. Basic dimensions of folded plates

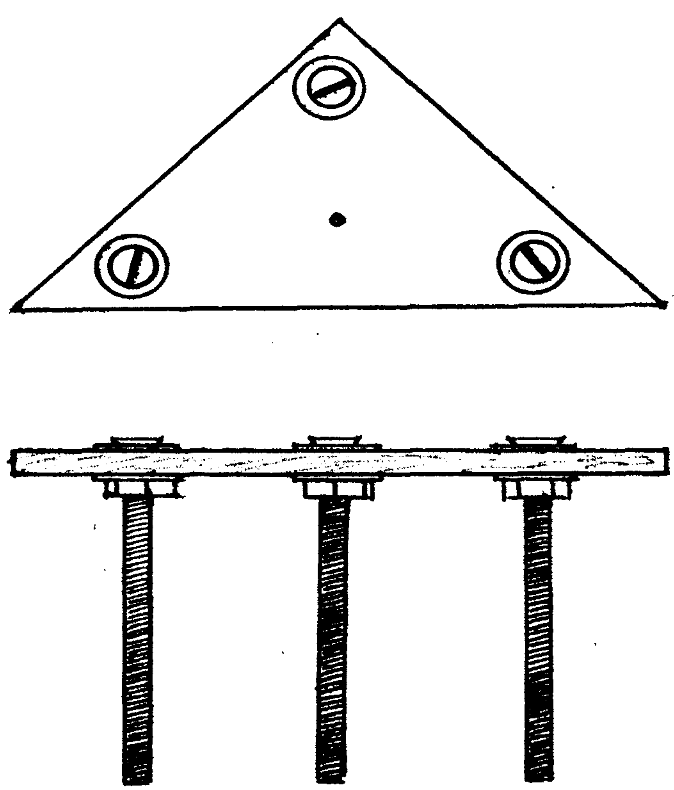

Figure 2. Loading triangle

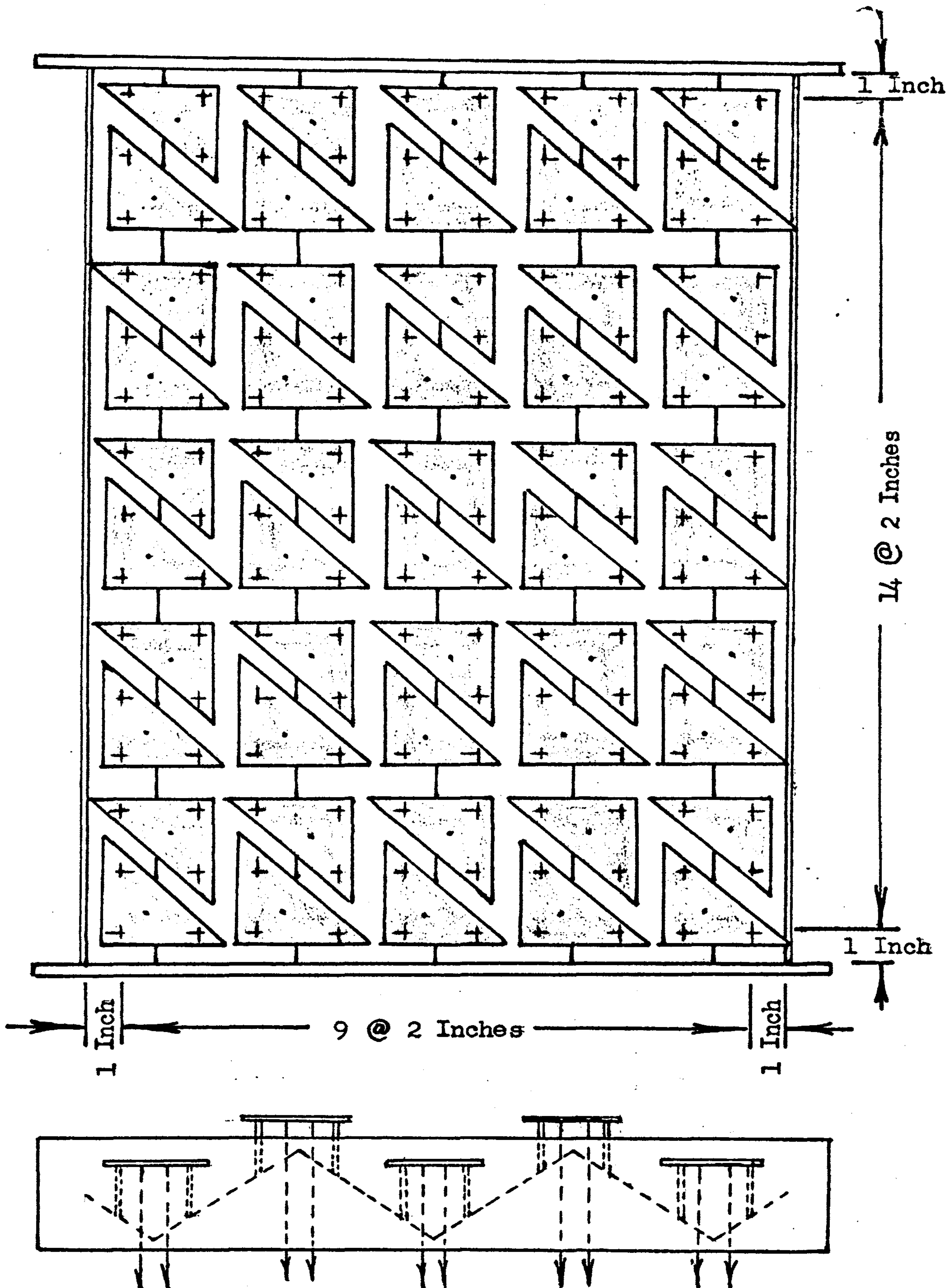

Figure 3. Loading positions for Model

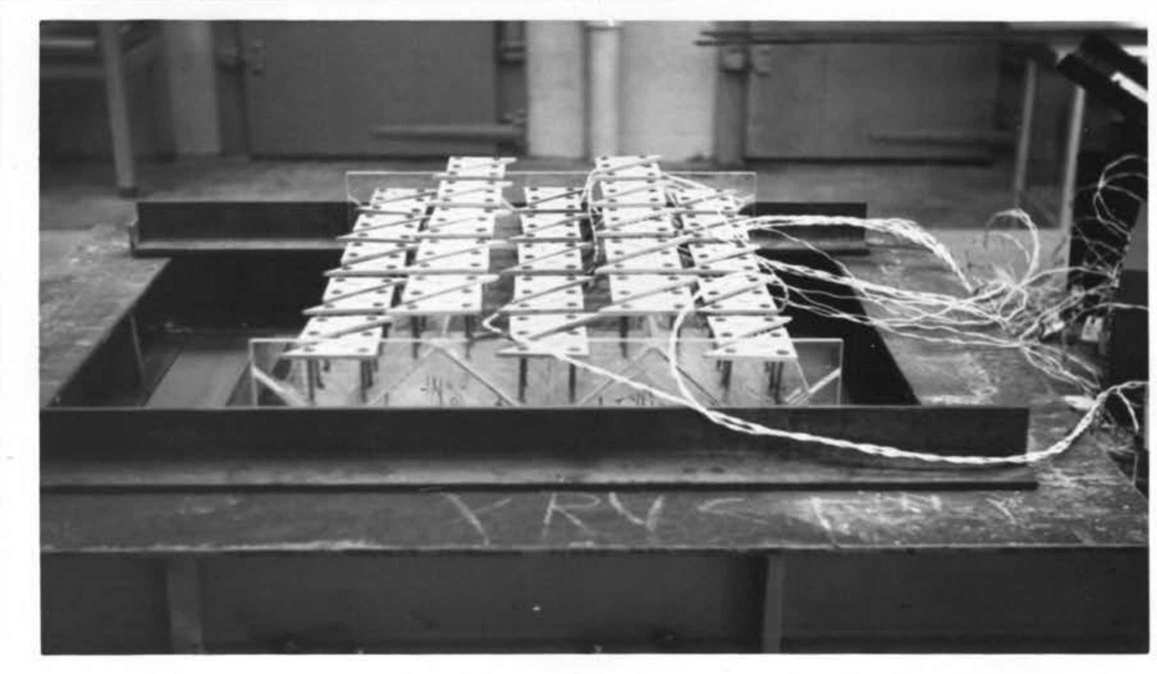

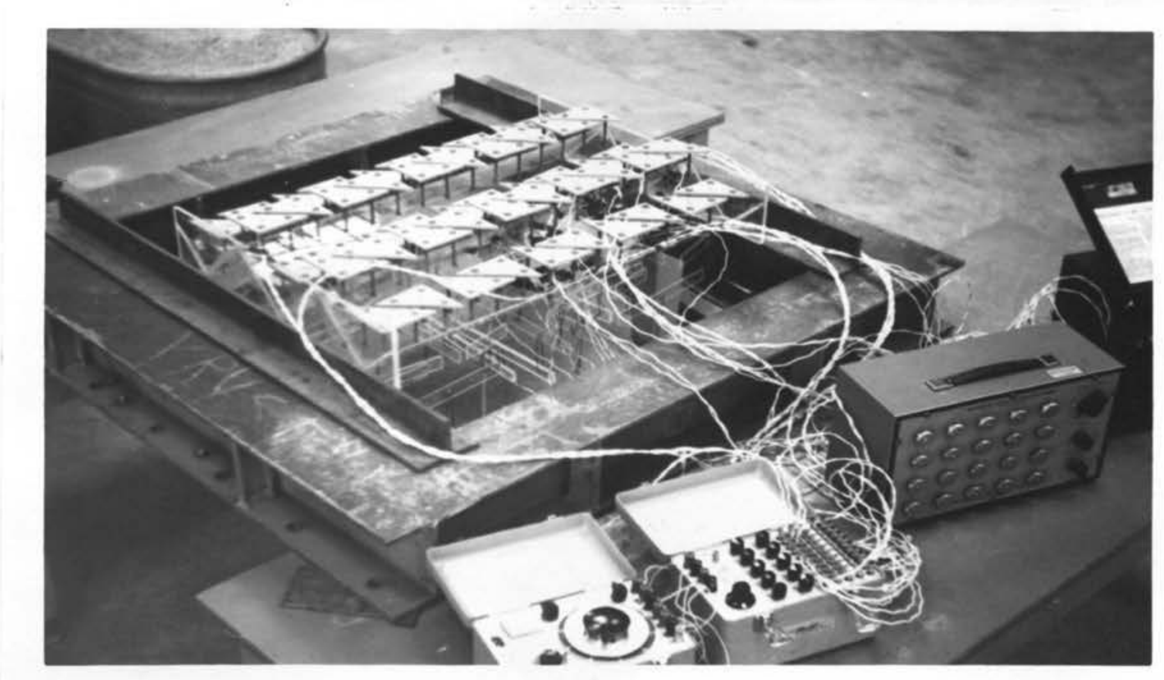

Figure 4. Model under load

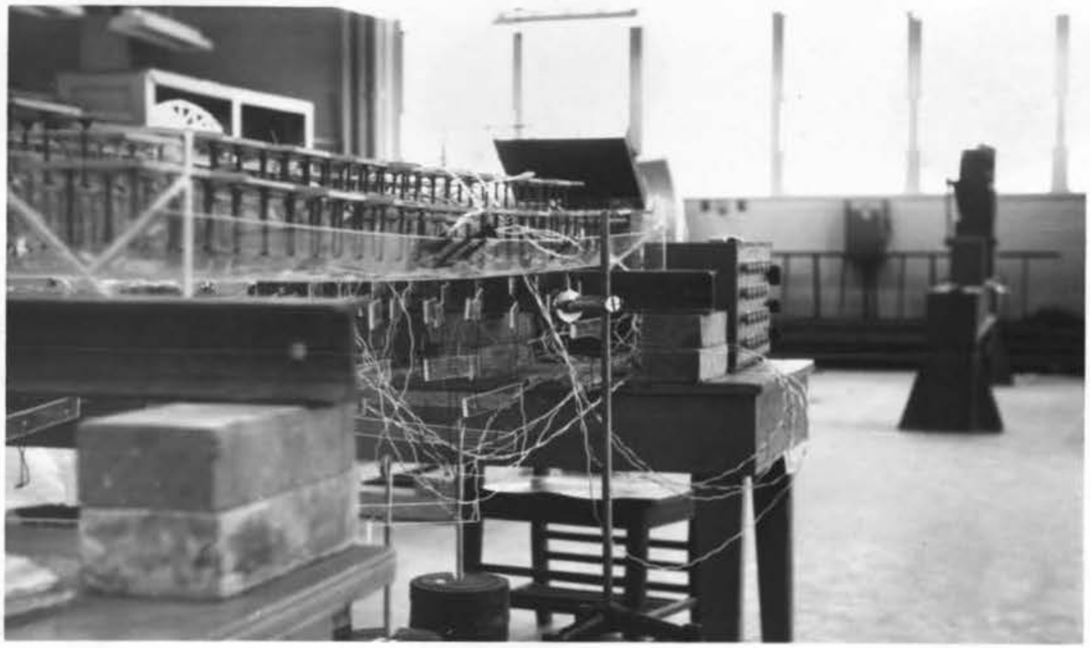

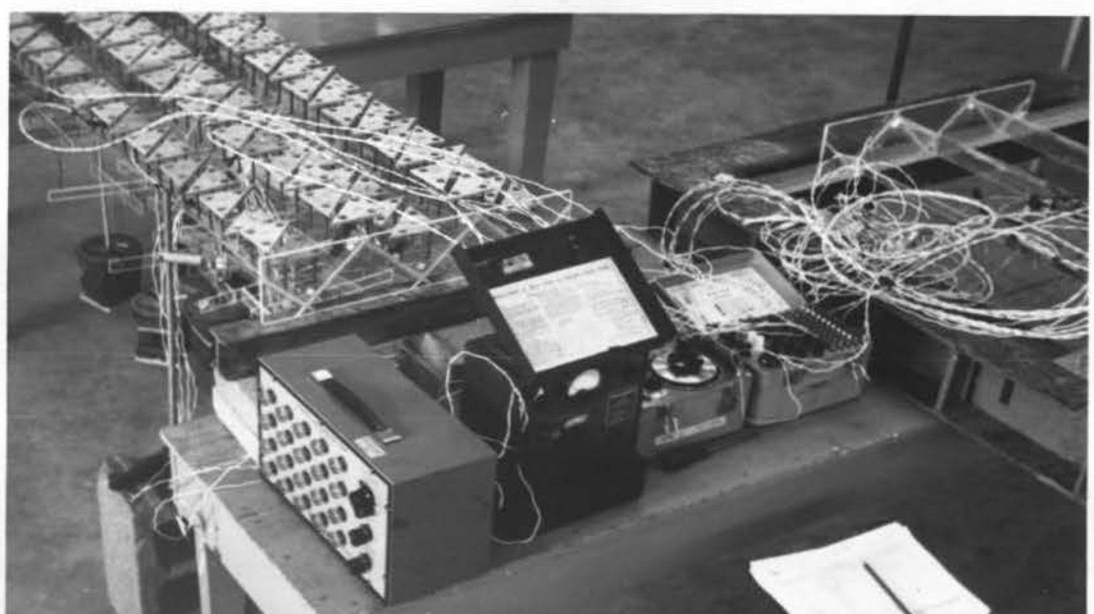

Figure 5. Prototype I under full load

manner than the other two plates. Instead of the triangles being placed on top of the folded plate, they were hung below it, achieving the same effect (Figure 6).

The strain gages used were SR-4 A-7's and A-1 rosettes. They were glued to the roof structure in the locations shown in Figure 7. The instrumented portion of the structure, which amounted to 1/4 of the folded plate, is shown in Figure 1. Since the roof was symmetrical, the strains in any other quarter were the same. It was felt that the small holes in the plates did not appreciably effect the strain readings since none of them were closer than 1 inch from a gage.

C. Testing

The testing procedure consisted of applying loads to the roof in increasing increments and recording the strain readings of each gage at each load. All the gages were zeroed at the same reading so that balancing could be accomplished without changing the dial settings on the Wheatstone bridge for each gage. Because of the number of gages, two bridges and two terminal boxes were used as shown in Figure 5. One system was used for the rosette gages and the other for the single gages.

Strain readings were taken approximately ten minutes after each increment of load was applied (Appendix 1). The loading increments for the model were 17 grams/inch^2

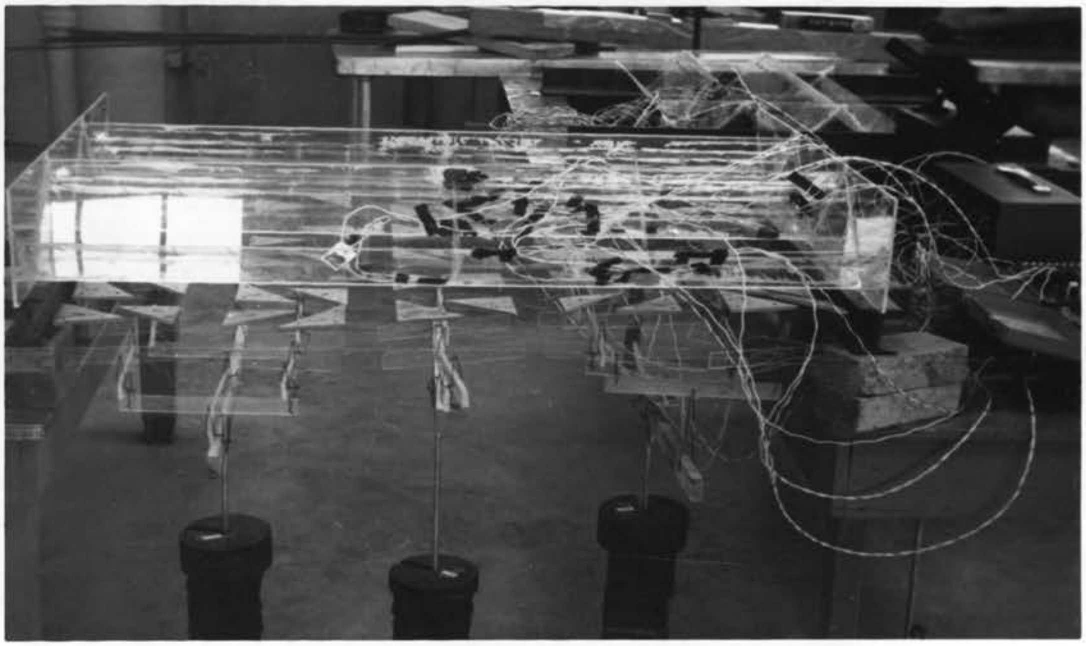

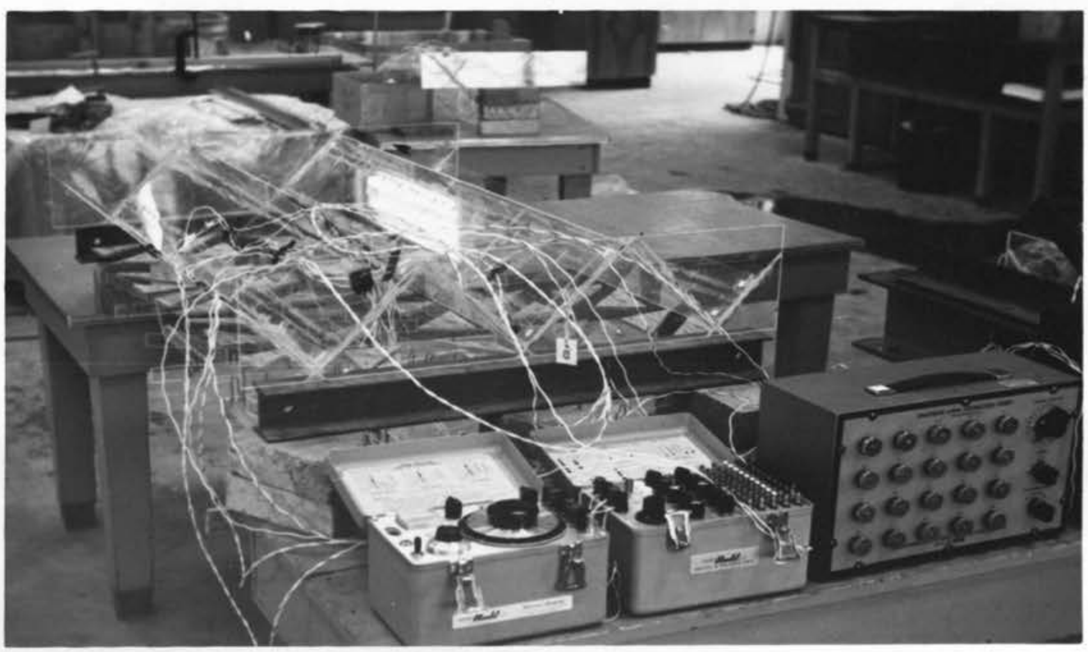

Figure 6. Prototype II being tested

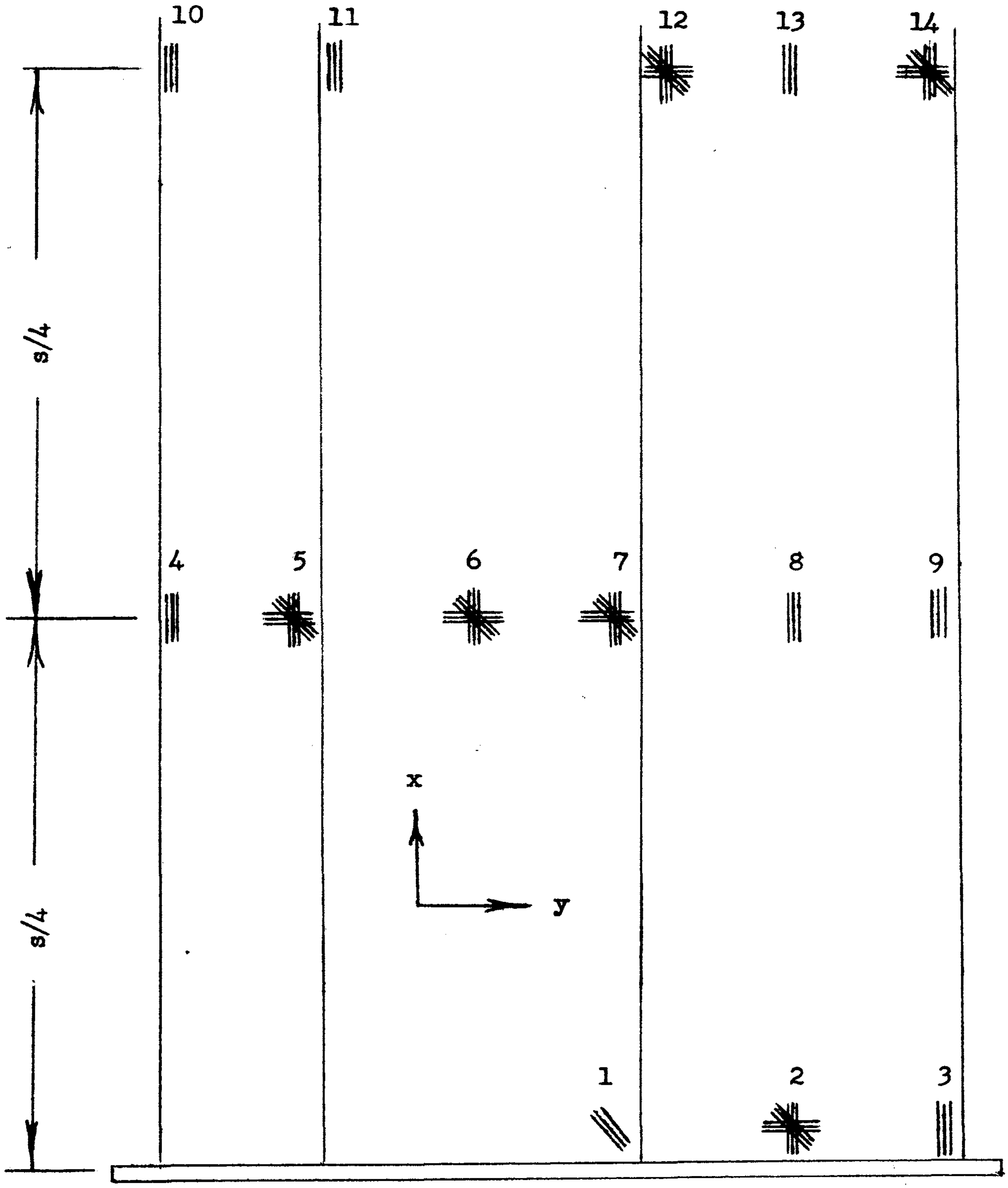

Shaded area of Figure 1

Figure 7. Strain gage locations and designation

to a total load of 110 grams/inch^2. Prototype I was loaded in increments of 9 grams/inch^2 to a total load of 70 grams/inch^2. For prototype II a maximum of 40 grams/inch^2 was reached.

In addition to loading the model and prototypes in increments, they were loaded with a small stabilizing load and then a large load, and the difference in strain recorded. This was done to see if the rate of loading or the size of loading increments had an effect upon the stress values. It was found that the size of loading increments had a small effect upon the slope of the load-strain curves, such as those shown in Figure 8. This was not enough to cause an appreciable error, even if one folded plate was not loaded with the same increments as another.

During the loading of the structure it was observed that the plexiglas would creep considerably for several minutes after a load was applied. This had been expected.

IV. RESULTS

A. Computations

The computations involved consisted of predicting the stresses in the prototypes through the use of the equations derived from dimensional analysis, converting the SR-4 strain readings to the true strains, and using these strains to determine the actual stresses in the model and prototypes.

Using the principle of part II, the stresses in the prototypes were predicted. For the locations at midspan and quarter points the equation, $\sigma = \frac{\lambda s^2 c I_m \sigma_m}{\lambda_m s_m^2 c_m I}$, was used. For prototype I this became $\sigma = \frac{(1)(2)^2(1)(1540)}{(1)(1)^2(1)(1287)}\sigma_m$. The ratio of 1540 to 1287 was used for the ratio of I_m to I because of the variance in the thickness of the plexiglas. Therefore $\sigma = 4.78\,\sigma_m$. Working with prototype II,

$$\sigma = \frac{(1.5)(1.5)}{(1)(1)}\frac{(1.5)}{(1)(1.5)}\frac{(127)}{(118)}\sigma_m,$$

$$\sigma = 1.67\,\sigma_m.$$

For stresses near the diaphragm, where shear was the principle factor, $\sigma = \frac{s\, t_m \sigma_m}{s_m t}$ was used. For prototype I it became $\sigma = \frac{(2)(1)\sigma_m}{(1)(1)} = 2\sigma_m$. In the second prototype the result was $\sigma = \frac{(1.5)(1)\sigma_m}{(1)(1)} = 1.5\,\sigma_m$.

To compare with the predicted stresses, the SR-4 strain gage readings were used to determine the actual stresses in the model and prototypes. A plot of load versus strain reading was made for each gage as shown in Figure 8. Each plot was a straight line and was corrected to zero strain at zero load so that for any load the corresponding strain could be taken from the curve. This was the apparent strain and will be referred to as "R".

For the single gage (A-7) it was necessary to assume that the apparent strain was the actual strain in the structure at the location of the gage and in the direction of the gage. In most cases the A-7 gages were placed where it was felt there would be little if any strain perpendicular to the gage's axis.

Knowing that $E = \sigma/\epsilon$, it was a simple matter to solve for the stress at any A-7 strain location by saying the actual strain, ϵ, = R. With the rosette gages, to determine the actual strains and stresses was somewhat more involved. The rosette gages were used at locations where it was not readily apparent in which direction the principal stresses would be acting. Their use not only enabled the principal stresses to be calculated, as well as their directions, but allowed the effect of lateral strain to be considered.

Corrections had to be applied to "R" to obtain the

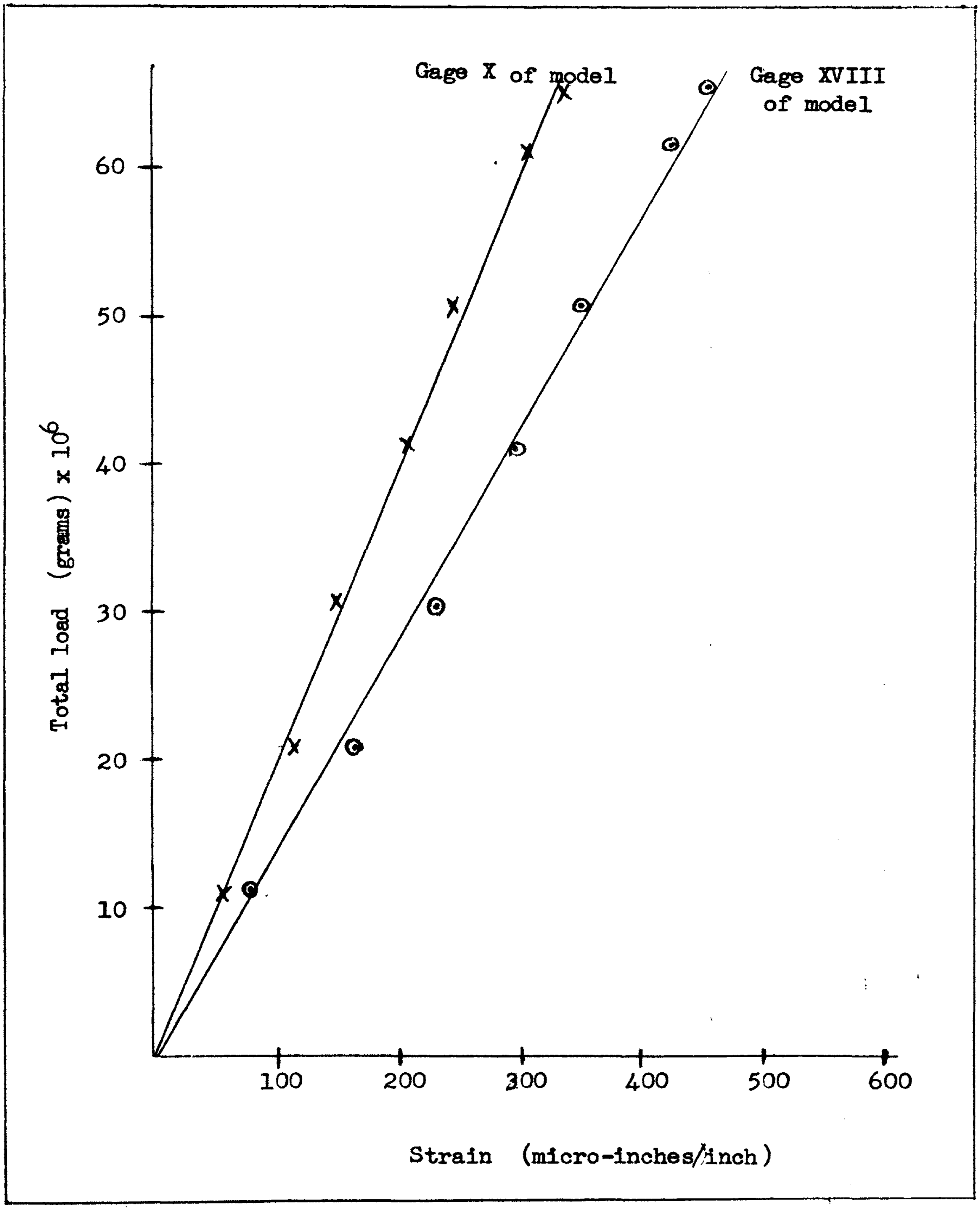

Figure 8. Sample load-strain curve for SR-4 gages

actual strain when using the rosette gages. The formulas used were

$$\epsilon_x = R_x - \frac{R_y}{b} \quad ,$$

$$\epsilon_{45} = 1.02R_{45} - \frac{R_x + R_y}{b} \quad , \text{ and}$$

$$\epsilon_y = R_y - \frac{R_x}{b} \quad ,$$

where the directions x, 45, and y are shown in the rosette gage sketched below.

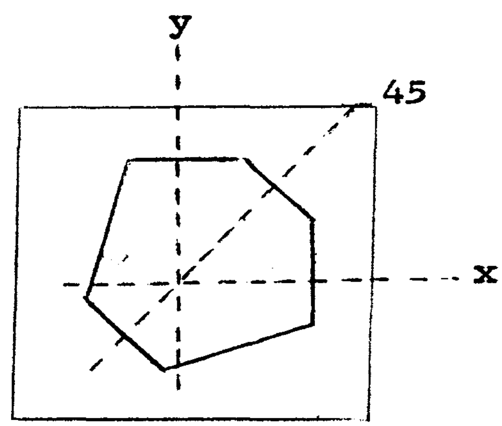

The symbol "b" is a constant for each lot of gages. It is determined by the gage manufacturer during the calibration of the gages.

Once the actual strains were known, the strains in the directions of the principal stresses were calculated as follows:

$$\epsilon_{1,2} = \frac{\epsilon_x + \epsilon_y}{2} \pm \sqrt{\left(\frac{\epsilon_x - \epsilon_y}{2}\right)^2 + \left(\frac{\gamma_{45}}{2}\right)^2}$$

where $\epsilon_{1,2}$ = the principal strains and $\gamma_{45} = 2\epsilon_{45} - \epsilon_x - \epsilon_y$.

The angle of rotation of the axes of the principal strains from the x-axis was given by

$$\phi = \frac{1}{2} \arctan \left(\frac{2(\epsilon_{45}) - \epsilon_x - \epsilon_y}{\epsilon_x - \epsilon_y} \right) ,$$

where a positive value represented counterclockwise rotation.

With the strains known, the stresses were computed using

$$\sigma_x = \frac{E}{1 - \mu^2}(\epsilon_x + \mu \epsilon_y) ,$$

$$\sigma_y = \frac{E}{1 - \mu^2}(\epsilon_y + \mu \epsilon_x) ,$$

$$\sigma_1 = \frac{E}{1 - \mu^2}(\epsilon_1 + \mu \epsilon_2) , \text{ and}$$

$$\sigma_2 = \frac{E}{1 - \mu^2}(\epsilon_2 + \mu \epsilon_1) .$$

B. <u>Comparisons</u>

The best way to compare the analytical, predicted, and experimental results is through the use of tables and graphs. The analytical stresses are those obtained using the method shown in Appendix 3. The experimental stresses are the actual stresses in the structure as computed from the strain readings. The predicted stresses come from the dimensional analysis equations previously derived, using the experimental stress in the model as σ_m.

In Table II appear the analytical and experimental stresses for various locations on the model with a load of 100 grams/inch^2. Table III compares the analytical, predicted, and experimental stresses for prototype I, while the same is shown for prototype II in Table IV.

Figures 9 and 10 give an indication of how closely the analytical and predicted stresses agree with the experimental results. The principal stresses at all the rosette gage locations were computed for all three approaches and are shown for prototype II in Figure 11.

Gage	Direction	Analytical Stress (p.s.i.)	Experimental Stress (p.s.i.)
1	45°	small	+51
3	x	0	+19
4	x	-274	-208
9	x	+164	+140
10	x	-370	-180
11	x	+295	+167
2	y	0	0
2	x	0	0
5	y	0	+129
5	x	+218	+130
6	y	0	-23
6	x	+18	-8
7	y	0	+77
7	x	-170	-95
12	x	-225	-195
12	y	0	-52
14	y	0	-50
14	x	+216	+136

Table II. Comparison of Stresses for Model

Gage	Direction	Analytical Stress (p.s.i.)	Predicted Stress (p.s.i.)	Experimental Stress (p.s.i.)
1	45°	small	+102	+138
3	x	0	+38	+25
4	x	-1096	-988	-475
9	x	+656	+665	+530
10	x	-1480	-855	-624
11	x	+1180	+793	+790
12	x	-900	-812	-950
12	y	0	-267	-379
14	y	0	small	small
14	x	+864	+646	+764

Table III. Comparison of Stresses for Prototype I

Gage	Direction	Analytical Stress (p.s.i.)	Predicted Stress (p.s.i.)	Experimental Stress (p.s.i.)
1	45°	small	+77	+80
3	x	0	+29	+59
4	x	-411	-348	-380
9	x	+246	+234	+226
10	x	-555	-301	-395
11	x	+442	+279	+350
5	y	0	+217	+384
5	x	+327	+217	+436
12	x	-337	-286	-347
12	y	0	-87	-171
14	y	0	-84	-192
14	x	+324	+228	+231

Table IV. Comparison of stresses for prototype II

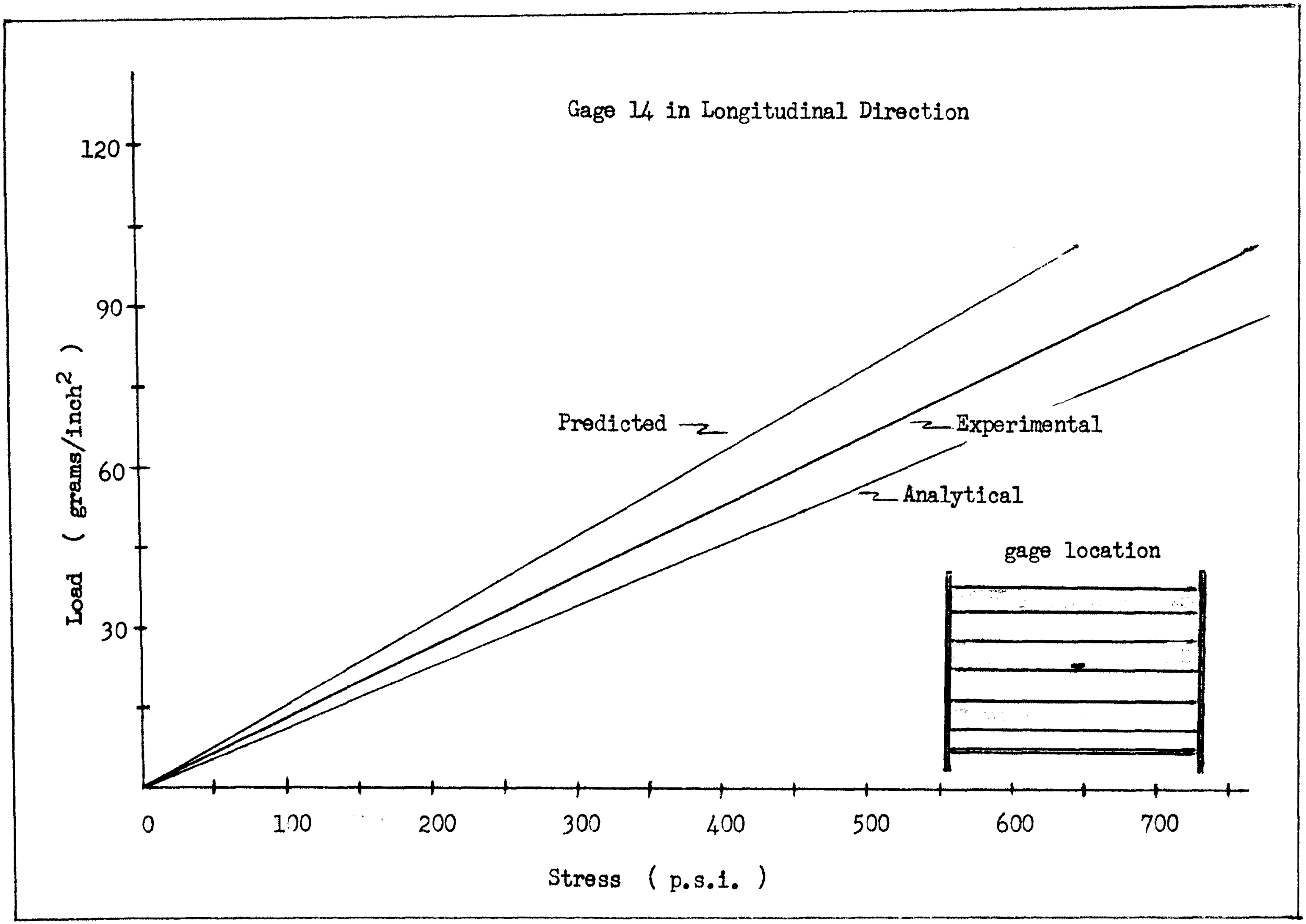

Figure 9. Comparison of analytical, predicted, and experimental stresses for prototype I

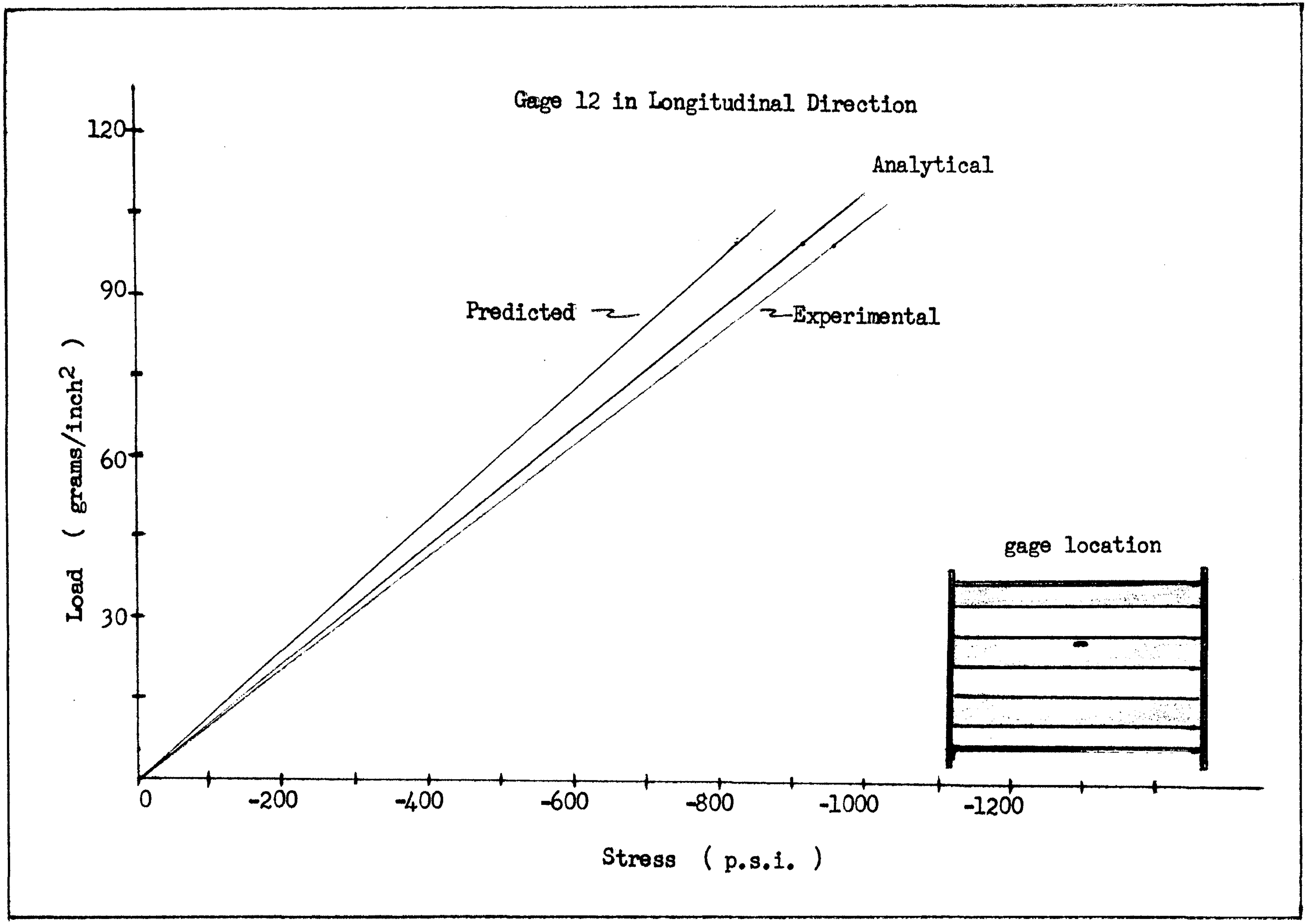

Figure 9. (Continued)

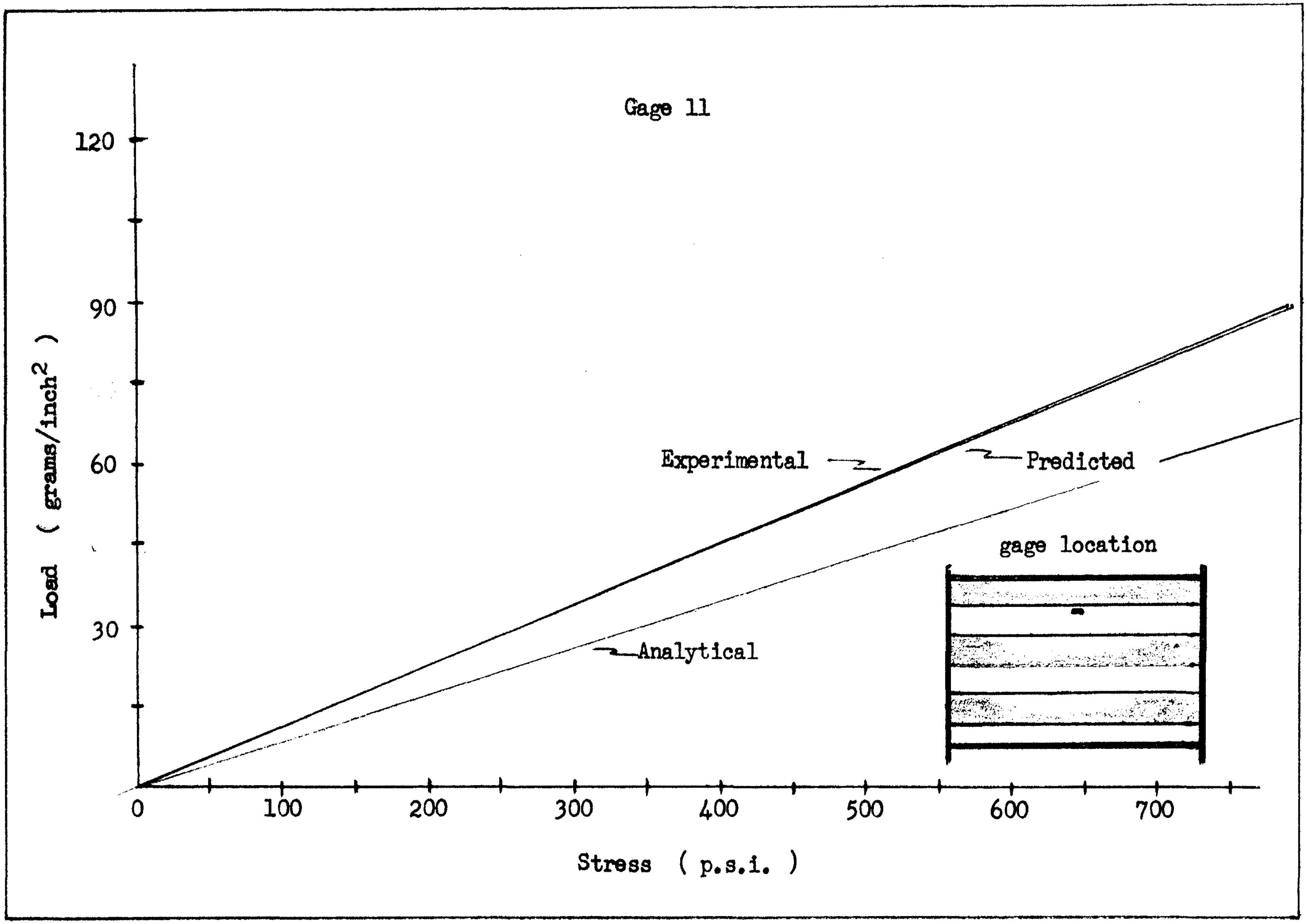

Figure 9. (Continued)

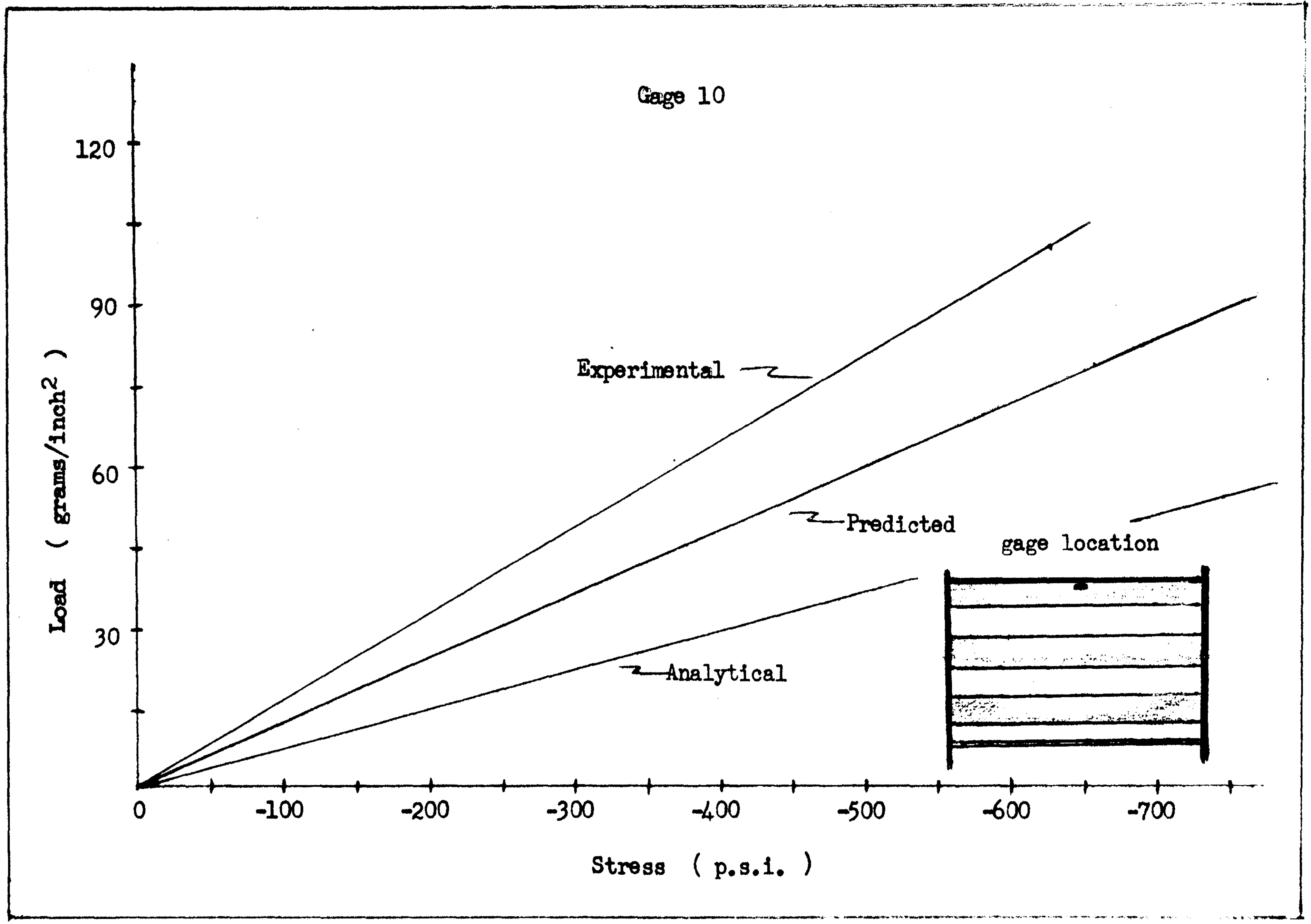

Figure 9. (Continued)

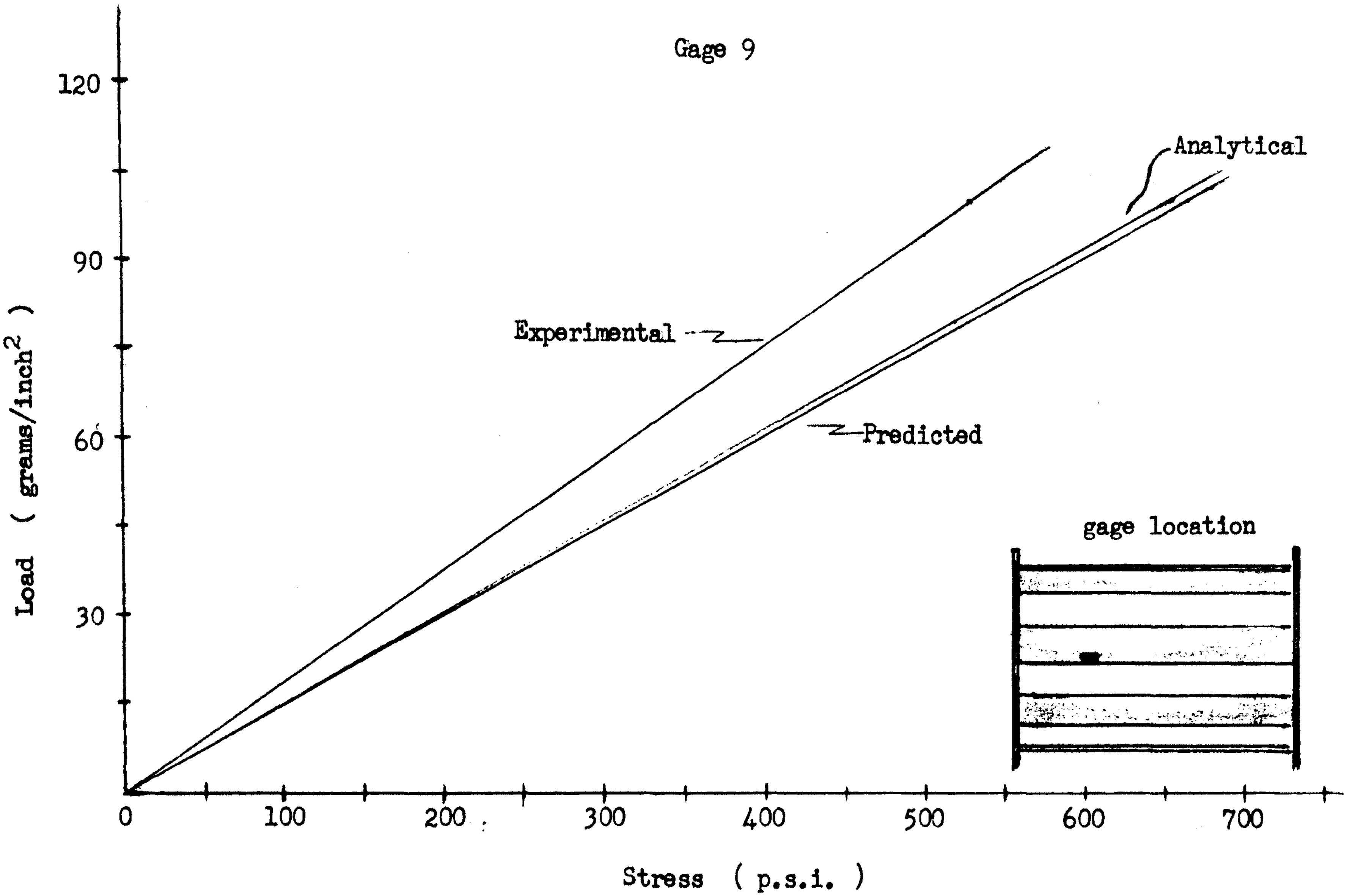

Figure 9. (Continued)

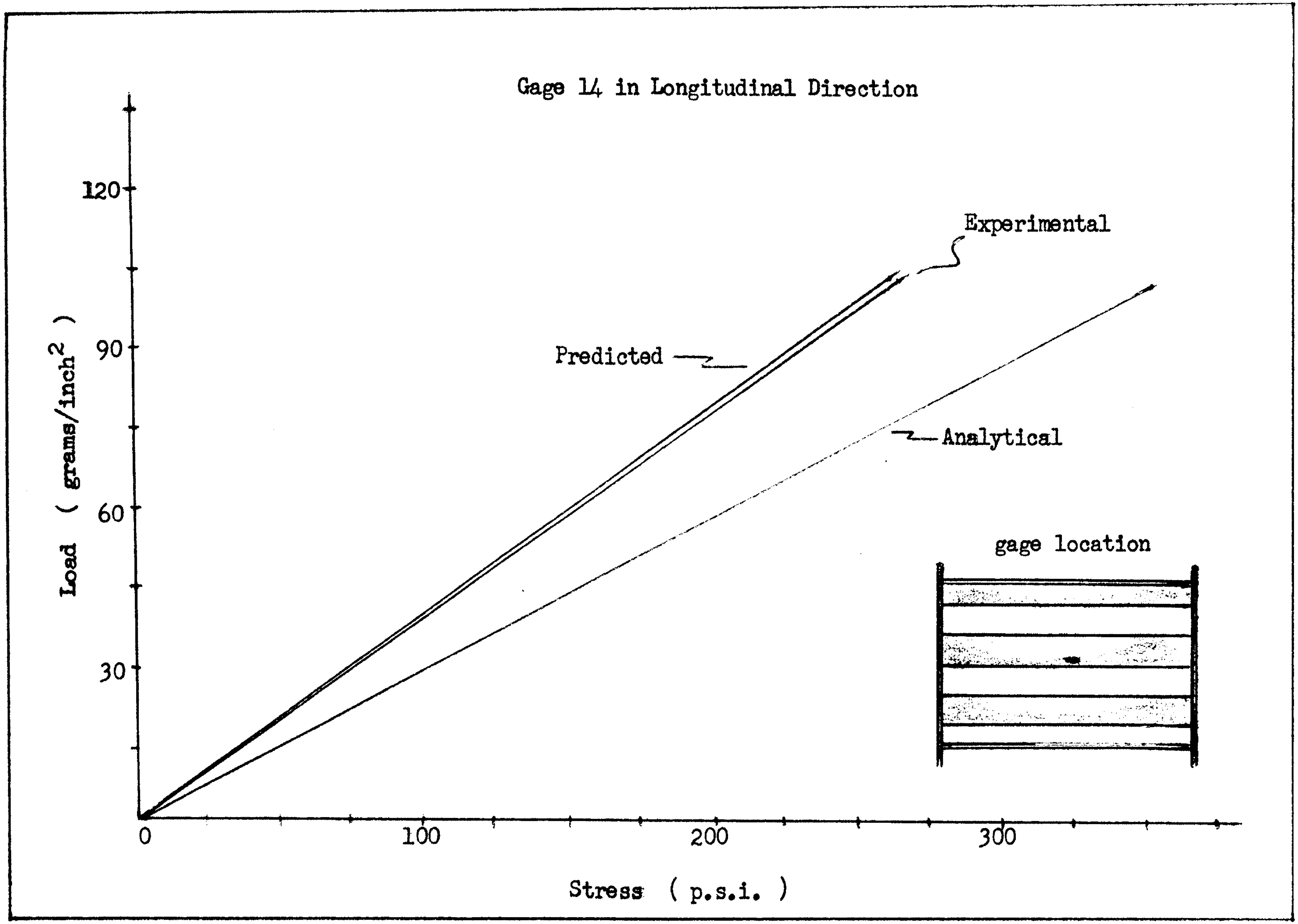

Figure 10. Comparison of analytical, Predicted, and Experimental Stresses for Prototype II

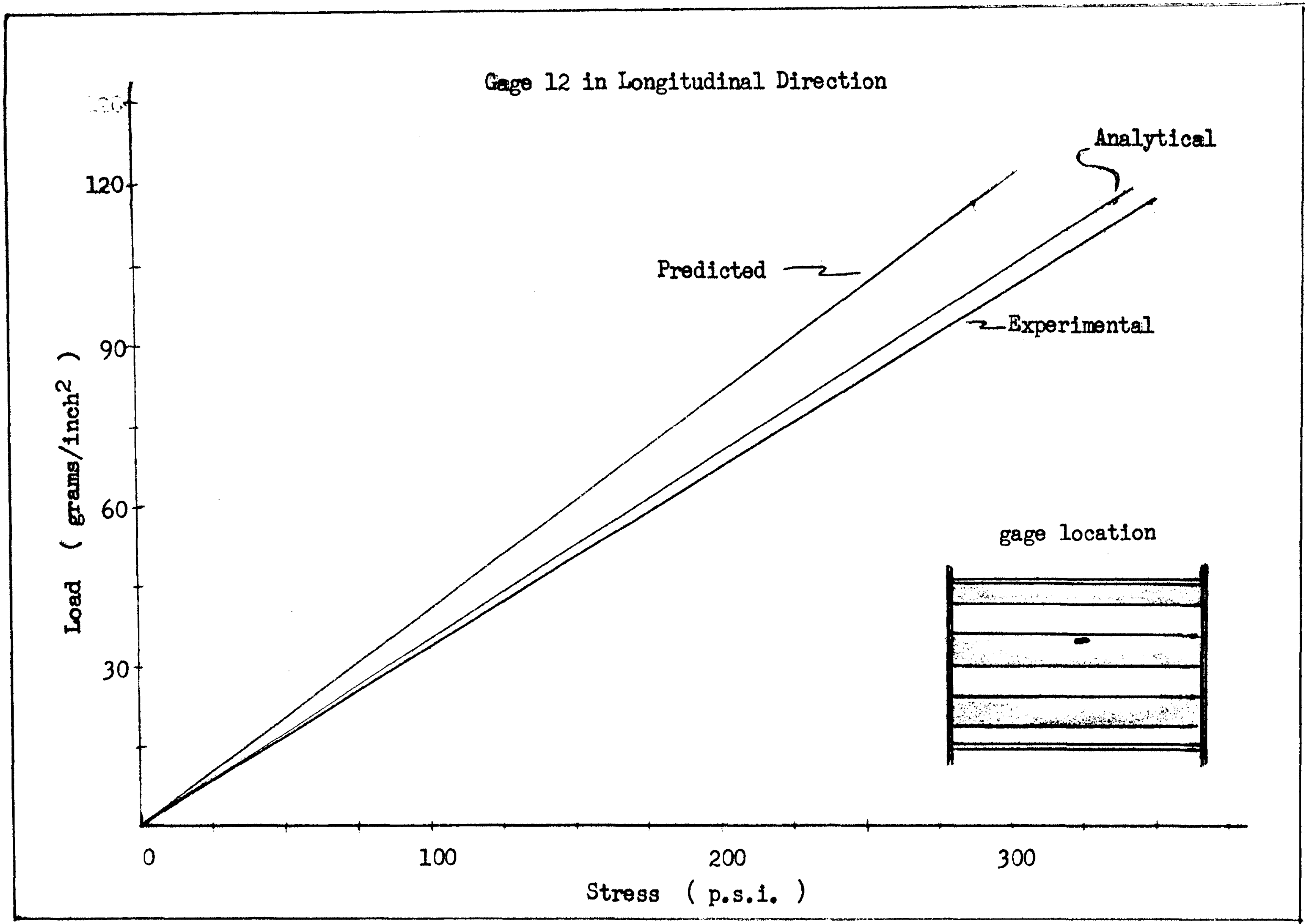

Figure 10. (Continued)

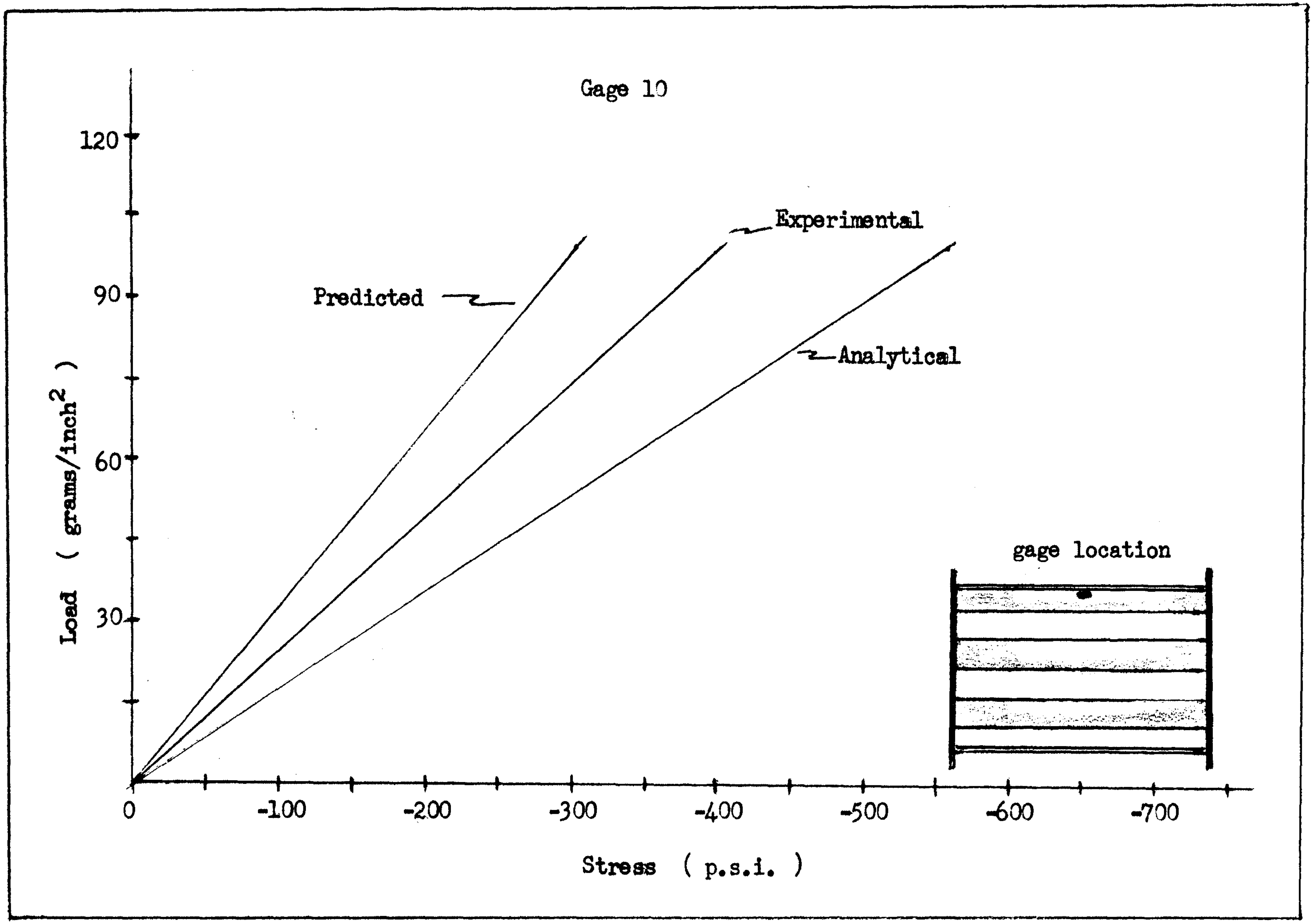

Figure 10. (Continued)

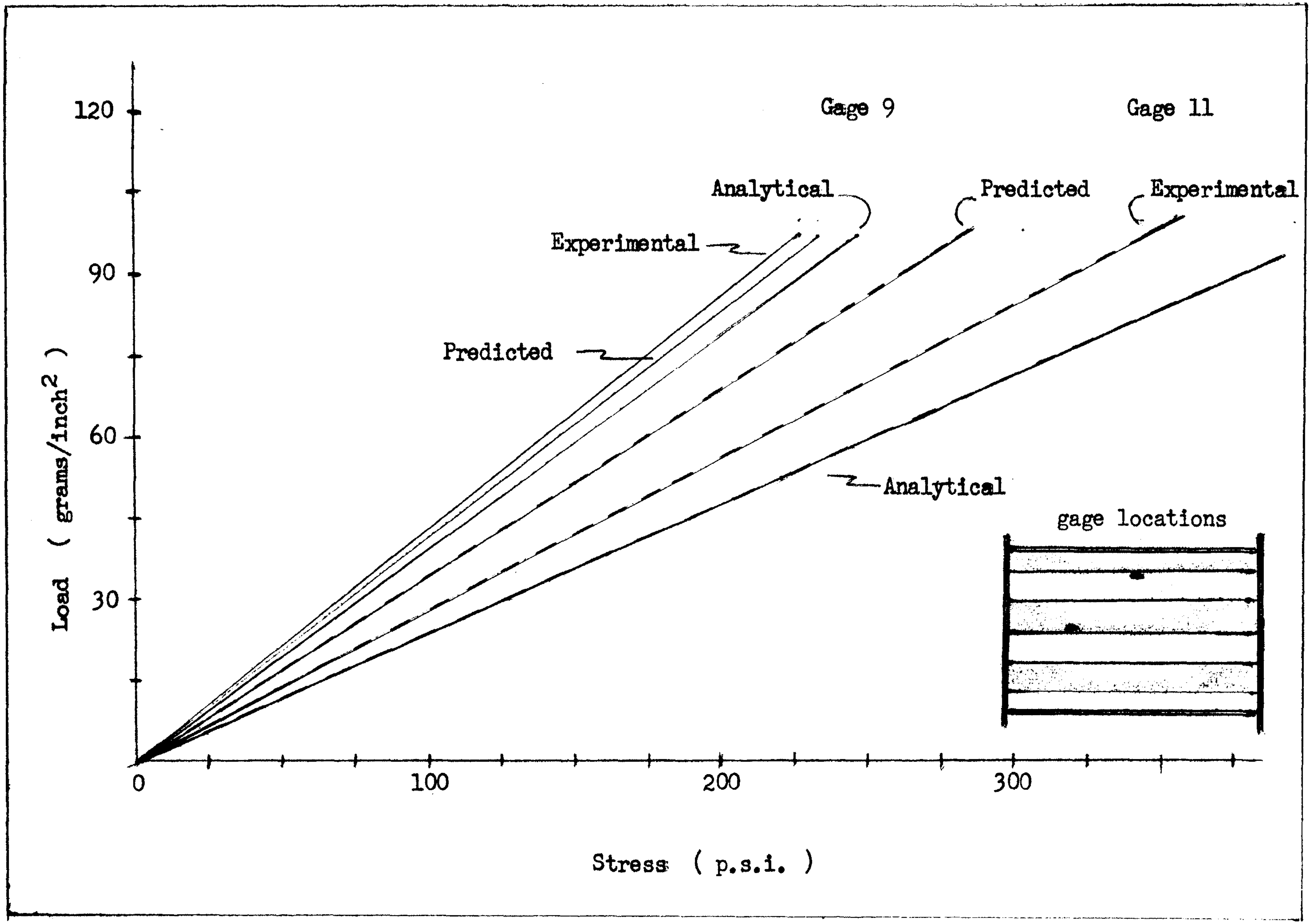

Figure 10. (Continued)

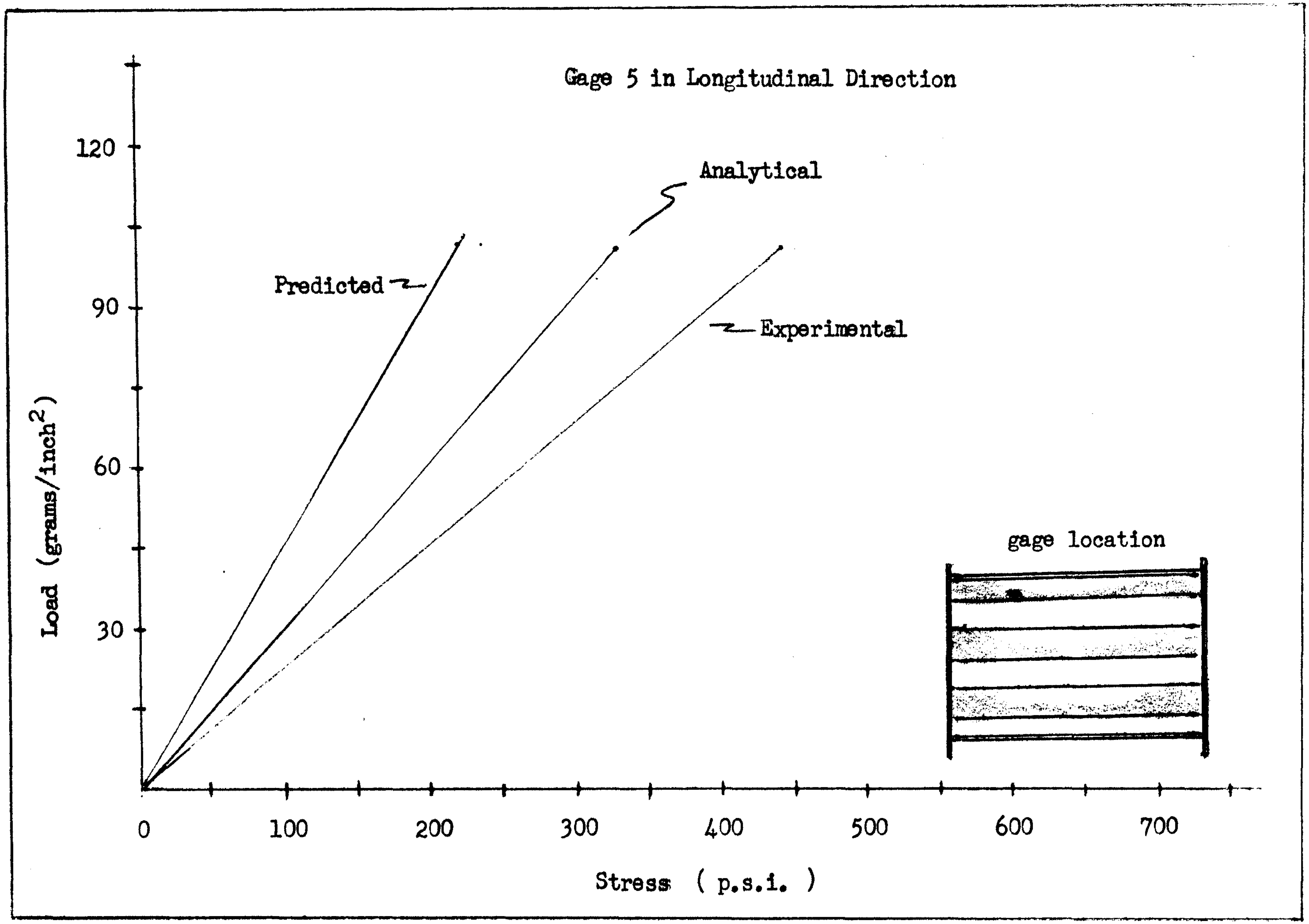

Figure 10. (Continued)

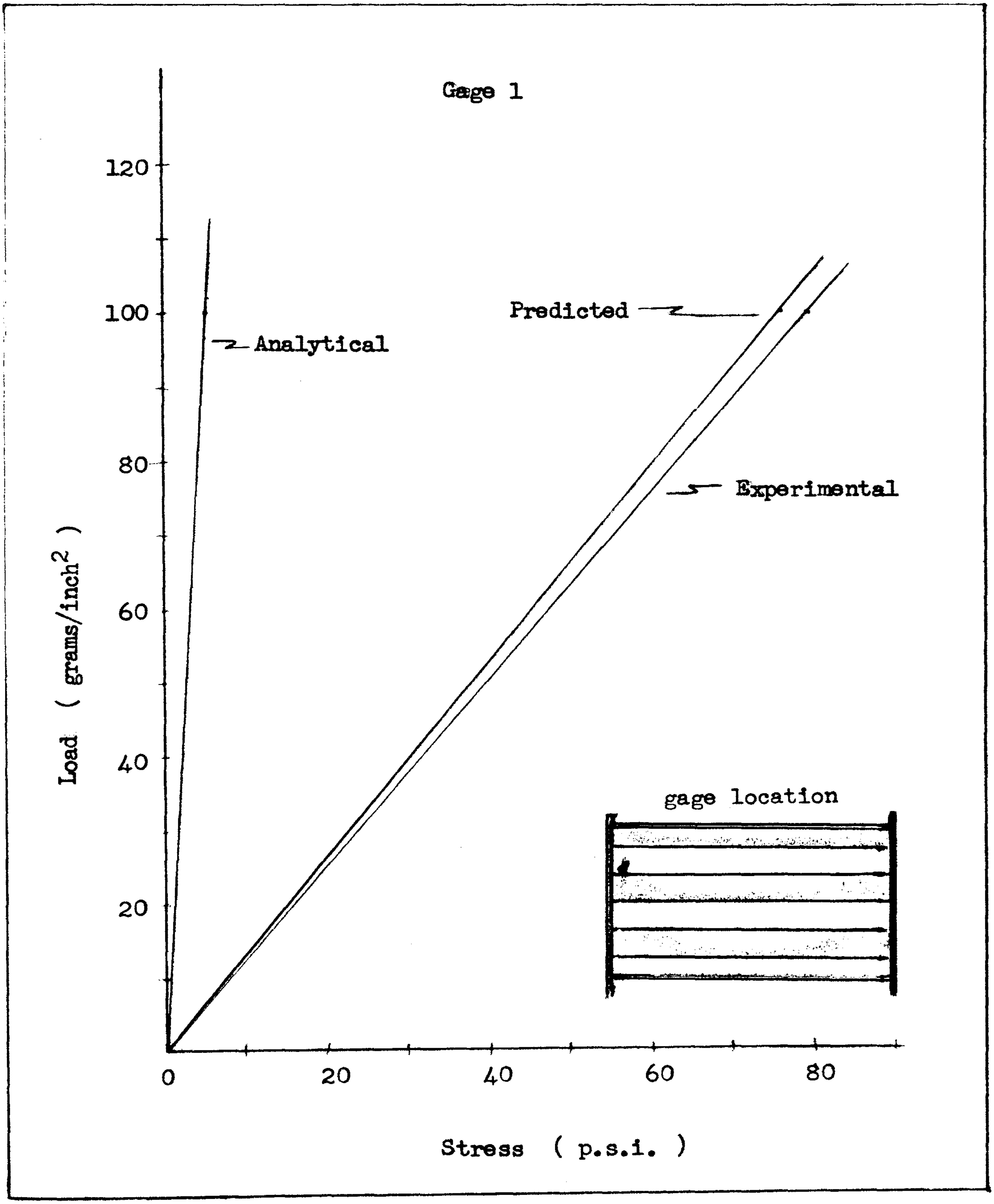

Figure 10. (Continued)

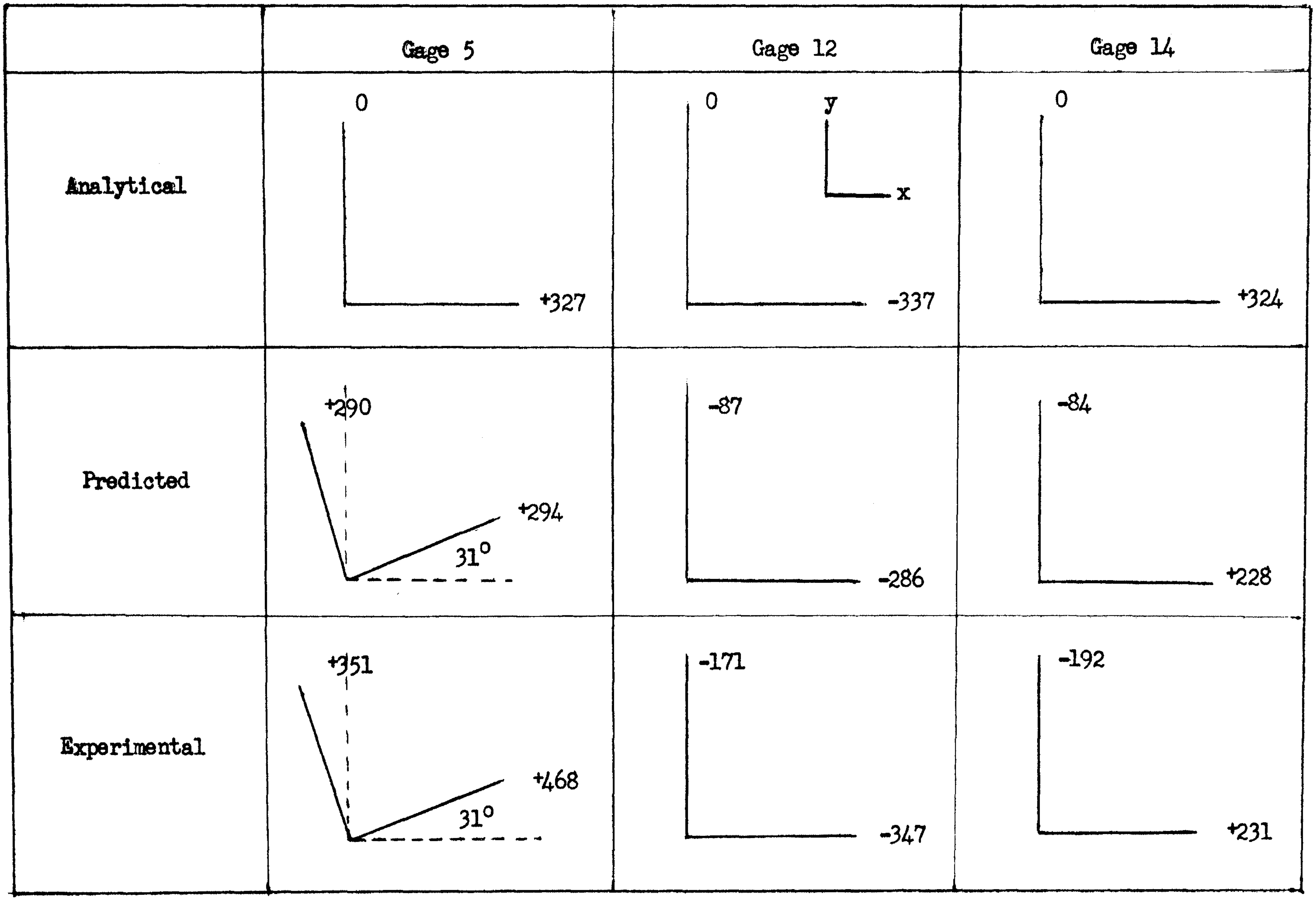

Figure 11. Comparison of principal stresses for prototype II

IV. CONCLUSION

The predicted stresses along the transverse centerline of the structure were in relatively good agreement with those found in testing the folded plates, thus indicating bending to be the major contributor to stress at that location. Near the end diaphragms where shear predominates, the predicted stresses were small and in fair agreement with the actual stresses.

At the longitudinal edge of the folded plate, especially at the quarter point, the greatest disagreement occurred. The analytical method gave values 67% greater than the actual longitudinal stress in the model at the location of gage 5. The transverse stress was of the same magnitude where the theoretical method showed it to be zero. At the same location in prototype II the transverse and longitudinal stresses were of similar magnitude, but 33% higher than the analytical and 100% higher than the predicted stress in the longitudinal direction. This indicates that there must be considerable transverse bending near the edge which is not accounted for analytically. There is also the possibility that some twisting of the edge plate takes place.

For the particular folded plates studied, the author would favor slightly the analytical approach over the model study as a method for designing. The predicted stresses were more accurate in places, but were usually lower than the actual stresses. As stated previously, neither method was in good agreement near the edge. Some of this discrepancy could be due to the material used for the folded plates.

It is suggested that plexiglas not be used as a material for model study. Even though it is easy to work with, it has several disadvantages. Young's Modulus was measured on several occasions and was found to vary up to 12% depending upon the humidity. A second problem is that the material creeps considerably. As it creeps the "E" also changes, making it difficult to obtain all strain readings at the same "E". To add to this, the thickness of the plexiglas sheets varies ±12% from the nominal thickness. A model using welded aluminum plates is a possibility.

In this particular model study it has been shown that the analytical approach can be used just as well and possibly more easily than models. It is the author's opinion though, that with a folded plate which is not symmetrical in cross-section, or which is other than simply supported, the model study is better. Besides this, a model study can be a valuable aid in developing new analytical approaches. By studying a model, the stress distribution in a particular plate is apparent, and from this there is an indication of what action is taking place.

BIBLIOGRAPHY

1. Born, Joachim (1962) Folded Plate Structures. Frederick Ungar, New York. p. 1 - 25.

2. Fialkow, M. N. (1962) Folded Plate Analysis by Minimum Energy Principle. ASCE Journal of St. Div. Vol. 88, ST3, p. 1 - 34.

3. Shaeffer, Ronald E. (1963) Model Analysis of Hyperbolic Paraboloid Thin Shell. Thesis, Iowa State University.

4. Murphy, Glenn (1950) Similitude in Engineering. Ronald, New York. 296 p.

5. Technical Data, Plexiglas, Mechanical Properties. 3rd. Ed., Rohm and Haas, Philadelphia.

6. Norris, Charles H. and Wilbur, John B. (1960) Elementary Structural Analysis. 2nd Ed., McGraw-Hill, New York. p. 593 - 594.

7. Traum, Eliahu (1959) The Design of Folded Plates. Proc. of ASCE Journal of St. Div. Vol. 85, ST3, p. 106 - 123.

8. Reiss, Max and Yitzhaki, David Analysis of Folded Plates. ASCE Transactions. Vol 129, p. 383.

9. Simpson, Howard (1958) Design of Folded Plate Roofs. ASCE Journal of St. Div. Vol 84, ST1, p. 1508 - 1521.

APPENDIX 1

The value of E, Young's Modulus, was determined by testing a cantilever beam of plexiglas taken from the same sheet as the material for the folded plates. The beam was approximately 1/2 inch by 1/8 inch, and had lengths of 6, 8, and 9 inches.

The beam was loaded at the end, as shown in Figure 12, and the deflections at the end recorded as increasing load was applied. A typical load-deflection curve is presented in Figure 13.

Plexiglas has the characteristic of creeping for several minutes after it is subjected to a load. Norris and Wilbur (6) have found that as the plexiglas creeps, Young's Modulus also changes until creep stops. Furthermore, they state that E will be the same for any load once the creep ceases. It is for this reason that there was a ten minute lapse after each load was applied before the deflection was read.

Using the load-deflection curve (Figure 13) and the following procedure, the value of Young's Modulus was calculated as 421,000 p. s. i.

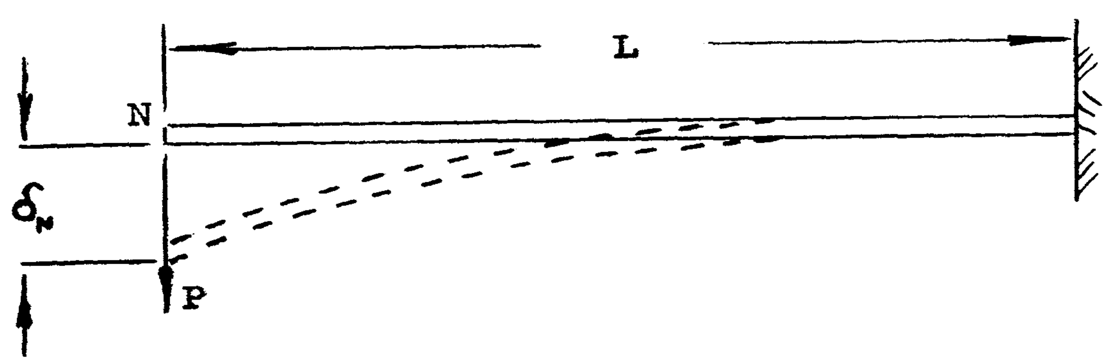

$$\delta_N = \frac{PL^3}{3EI} \text{ , and}$$

solving for "E": $$E = \frac{PL^3}{3\delta_N EI} \text{ ,}$$

where $\frac{P}{\delta_N}$ can be obtained from Figure 13.

P = load applied

L = length of cantilever beam

δ_N = deflection at point "N"

I = moment of inertia

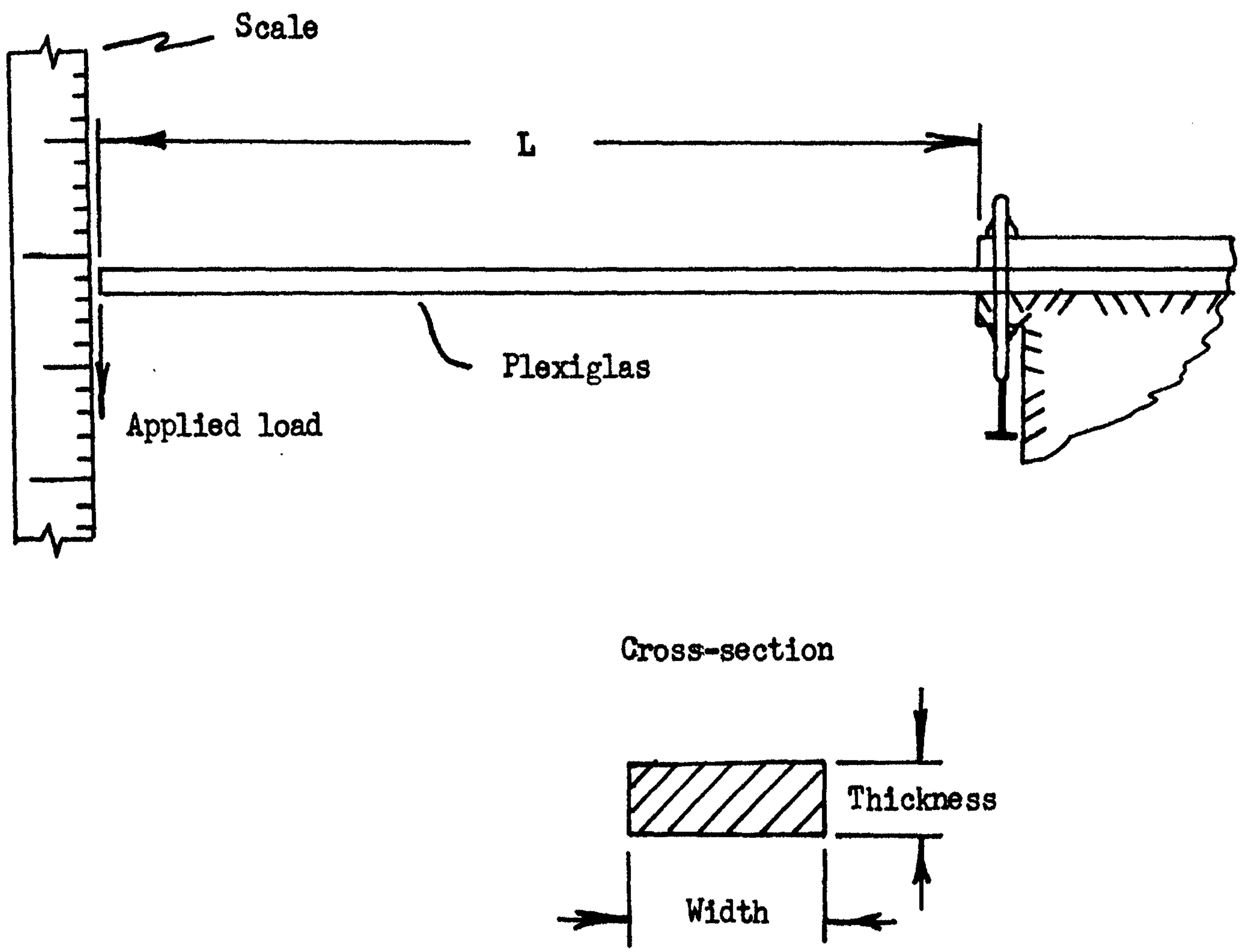

Figure 12. Laboratory set up for determining "E"

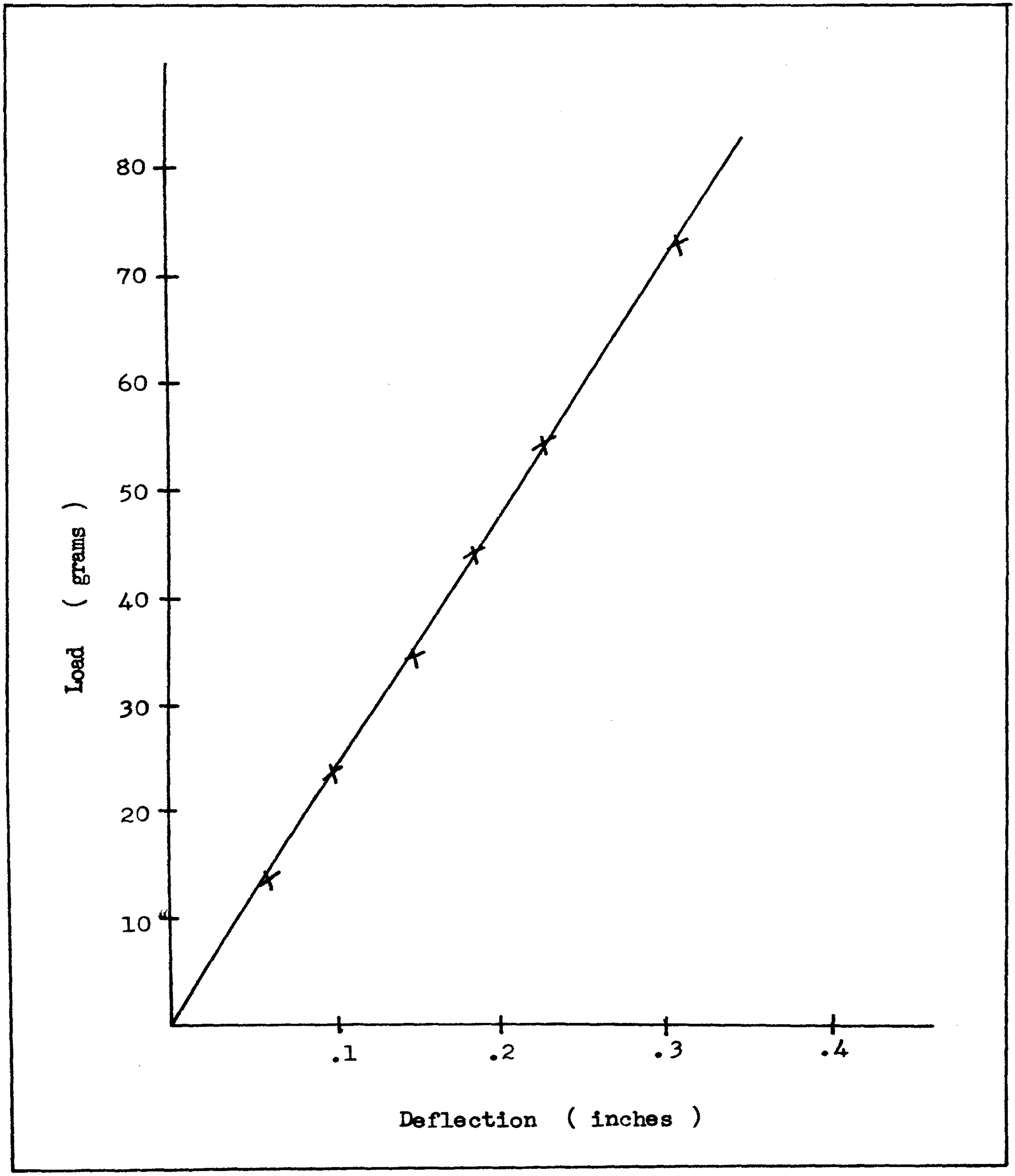

Figure 13. Load-deflection curve for plexiglas beam

APPENDIX 2

The value of μ, Poisson's Ratio, was determined by testing a rectangular column of plexiglas in tension. The column was approximately 1/2 inch by 1/8 inch, and 20 inches in length.

The column was loaded as shown in Figure 14. With increasing increments of load, the lateral and longitudinal strains were recorded. Figure 15 shows a typical lateral-longitudinal strain curve.

Knowing that Poisson's Ratio is the lateral strain divided by the longitudinal strain ($\epsilon_{lat.}/\epsilon_{long.}$), it is apparent that the slope of the curve of Figure 15 is μ.

The average value of μ for this specimen of plexiglas was 0.377.

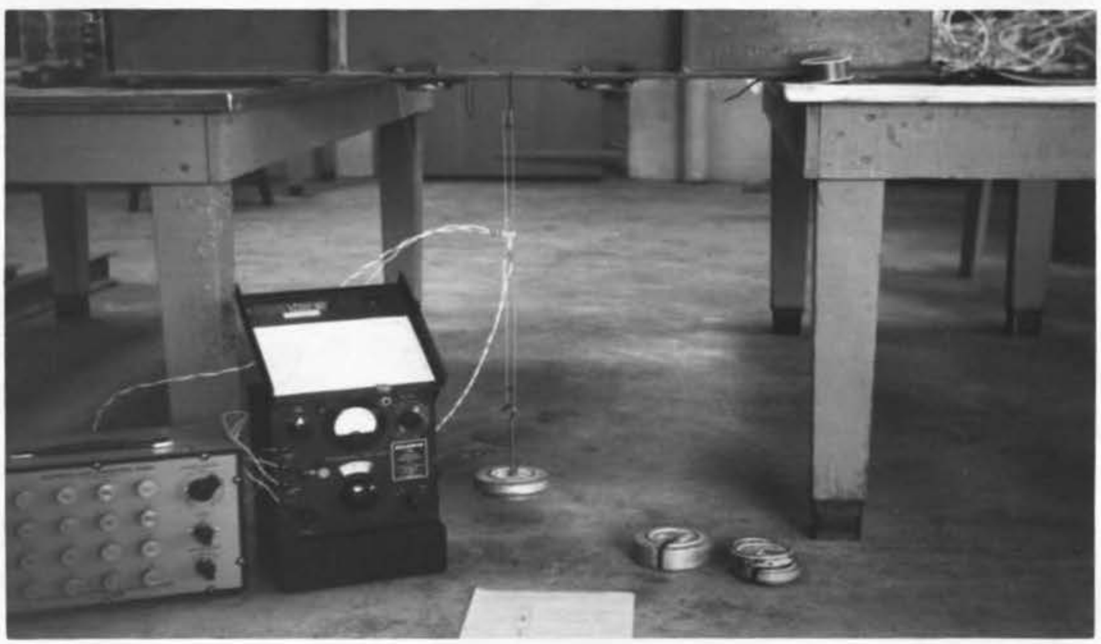

Figure 14. Testing for Poisson's Ratio

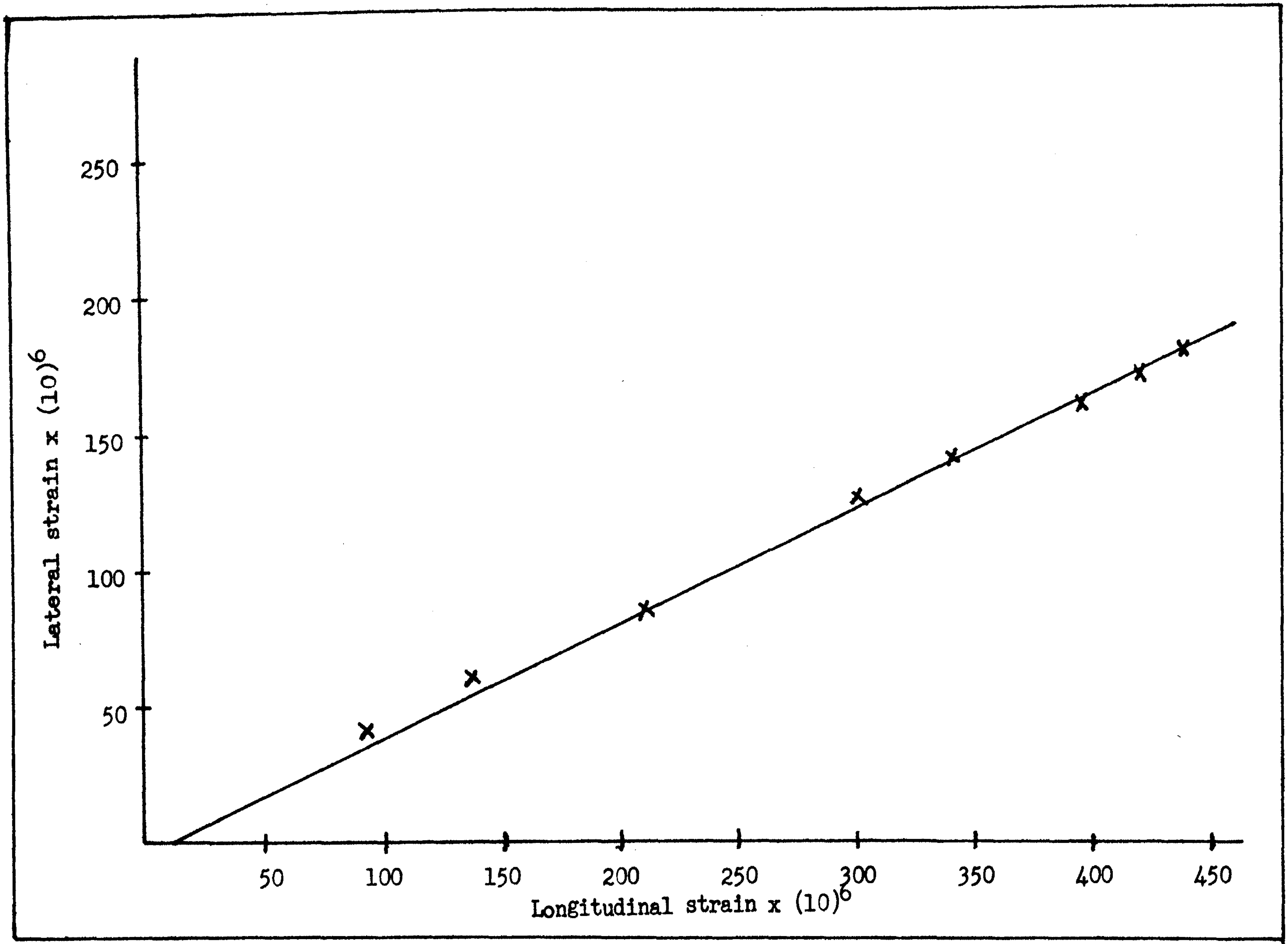

Figure 15. Lateral-longitudinal strain curve

APPENDIX 3

The analytical method employed to compute the stresses in the folded plates was the one developed by Born (1). It is a refinement of the bending theory approach and gives the same results as similar methods developed by Vlassow (7), Yitzhaki and Reiss (8), Simpson (9), and others. The calculations for the model with a load of 100 grams/inch^2 follows.

Folded Plate

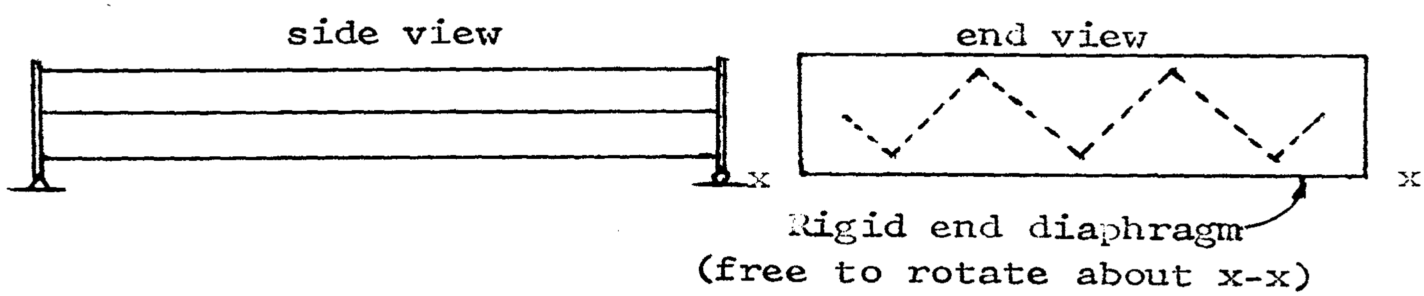

Transverse Cross-section

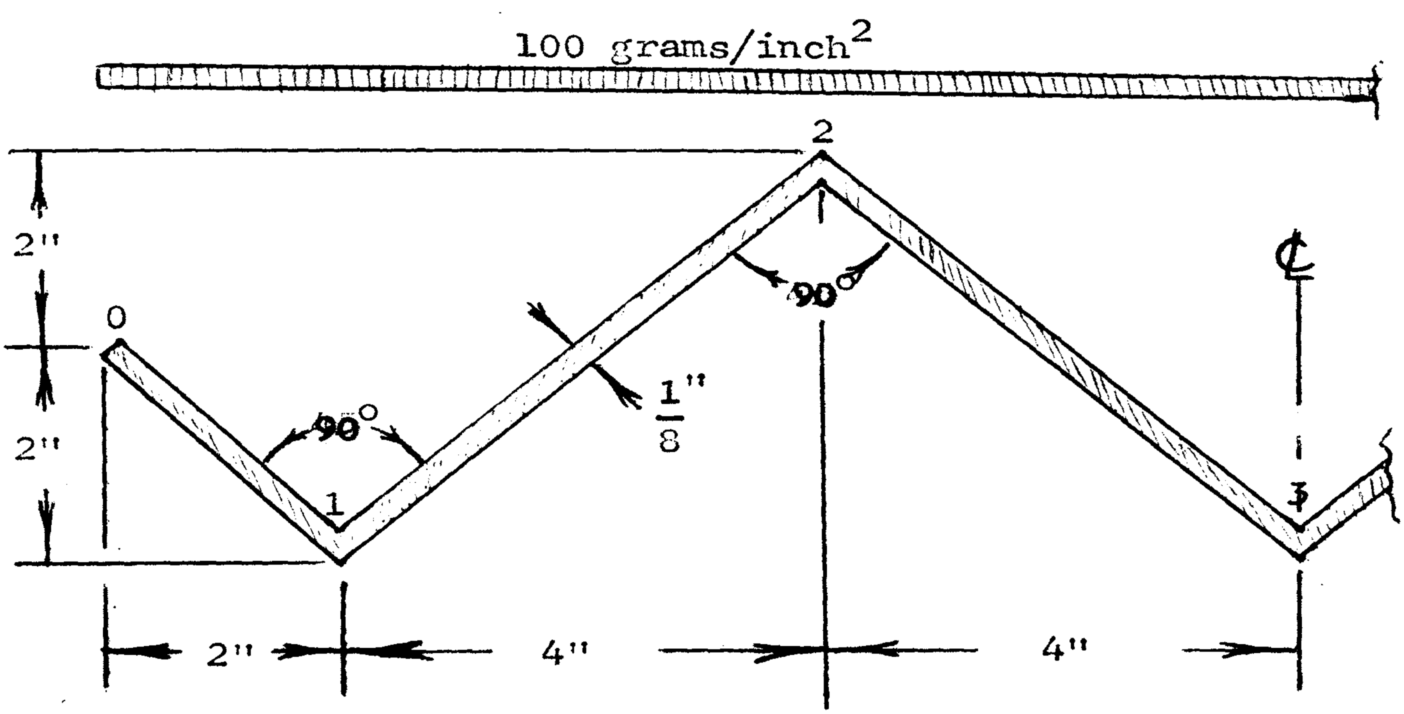

Elastic Properties of Plates Acting as Deep Beams
(Longitudinal Action)

Ridge	Plate	d in.	t in.	$A = d \cdot t$ in.^{2}	$S = td^2/6$ in.^{3}	$I = Sd/2$ in.^{4}
0						
	1	2.83	1/8	.354	.167	.236
1						
	2	5.66	1/8	.707	.667	1.890
2						
	3	5.66	1/8	.707	.667	1.890
3						

<u>First</u> <u>Step</u>: Slab Action (transverse) --- one inch strip

Take a one inch transverse strip of folded plate and assume supported as shown below. Use moment distribution to determine moments at the assumed supports.

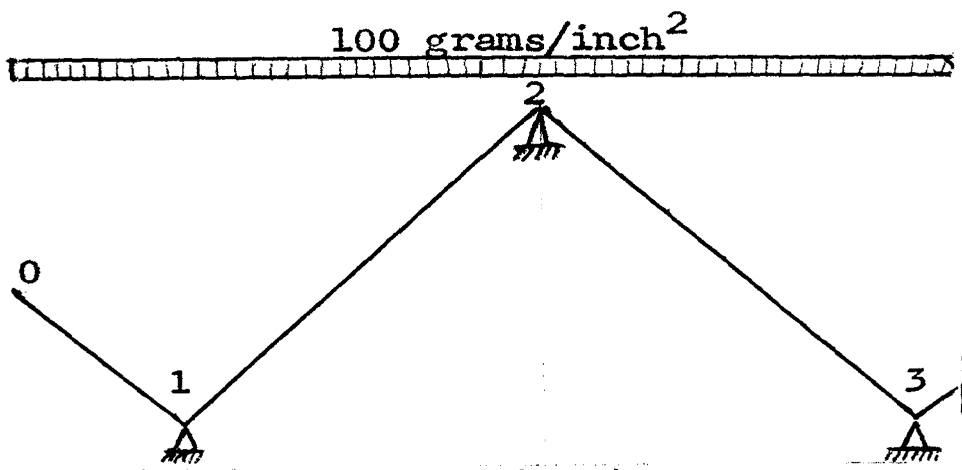

0	1	3/7	4/7	0	
+200	-133	+133	-133	+133	F.E.M. (in-gm)
	-67	-34			
+200	-200	+14	+19	+10	
		+114	-114	+143	Mom. at ridges

Reactions at assumed supports:

200	200	200	200	200	Due to load
	21.6	21.6	7.2	7.2	Due to Moment
200	222	178	193	207	Total

grams

Now assume the reactions are the loads at the ridges, but in the opposite direction. Break them up into their components parallel to the plates as shown.

Artifical Joint Restraints
(AJR)

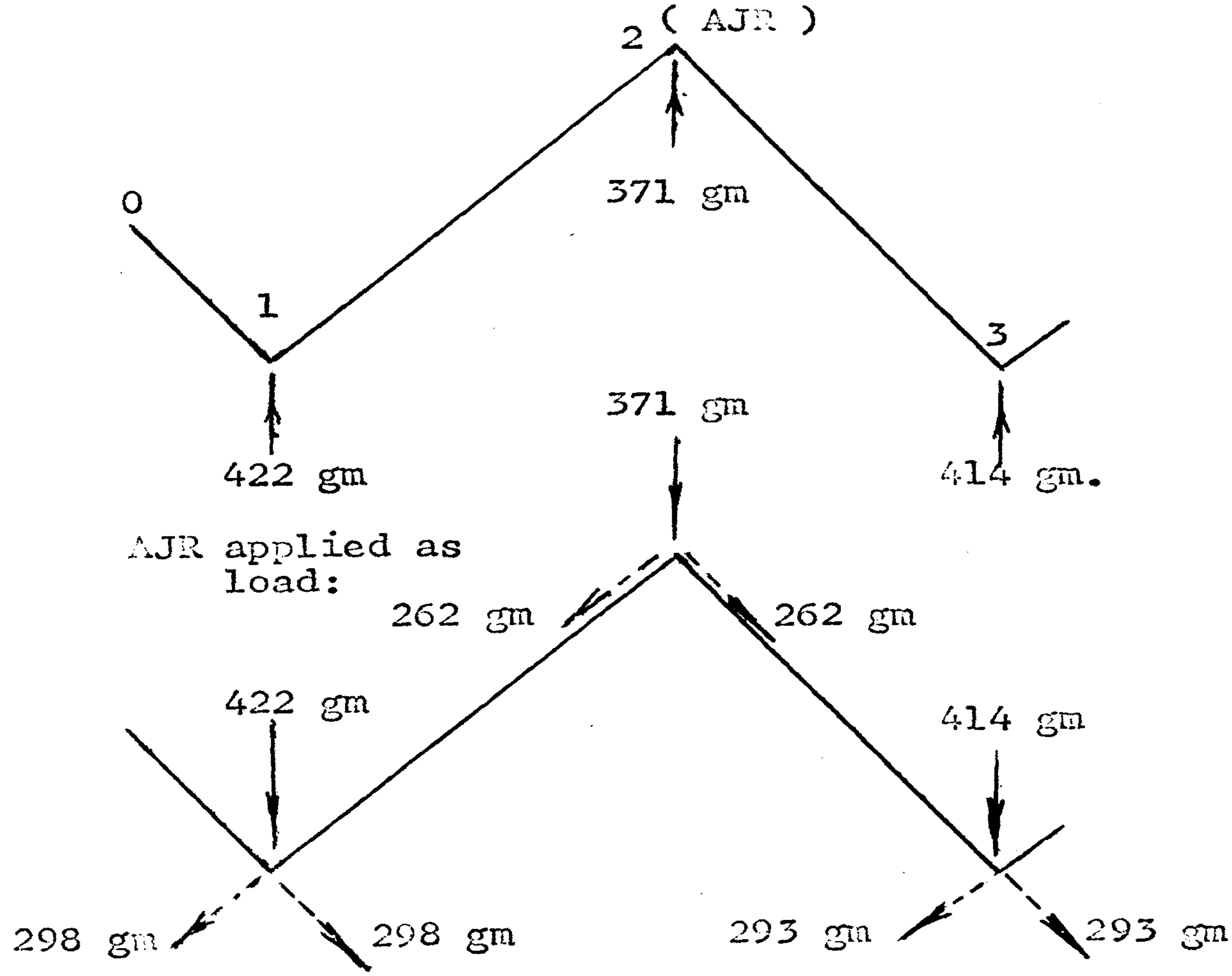

Second Step: Plate Action (longitudinal)

Sum up the preceding ridge loads for each plate and assume it is the uniform load acting on the plate. The uniform loads become 298 gm/in. for plate 1, 560 gm./in. for plate 2, and 555 gm./in. for plate 3. These cause bending stresses as shown below. They are computed for the center of the folded plate.

Where two adjacent plates join, the stress must be the same, but, considering bending only, we do not get this. Therefore, shearing forces "T" are assumed as shown and solved for later to make the adjacent stresses equal.

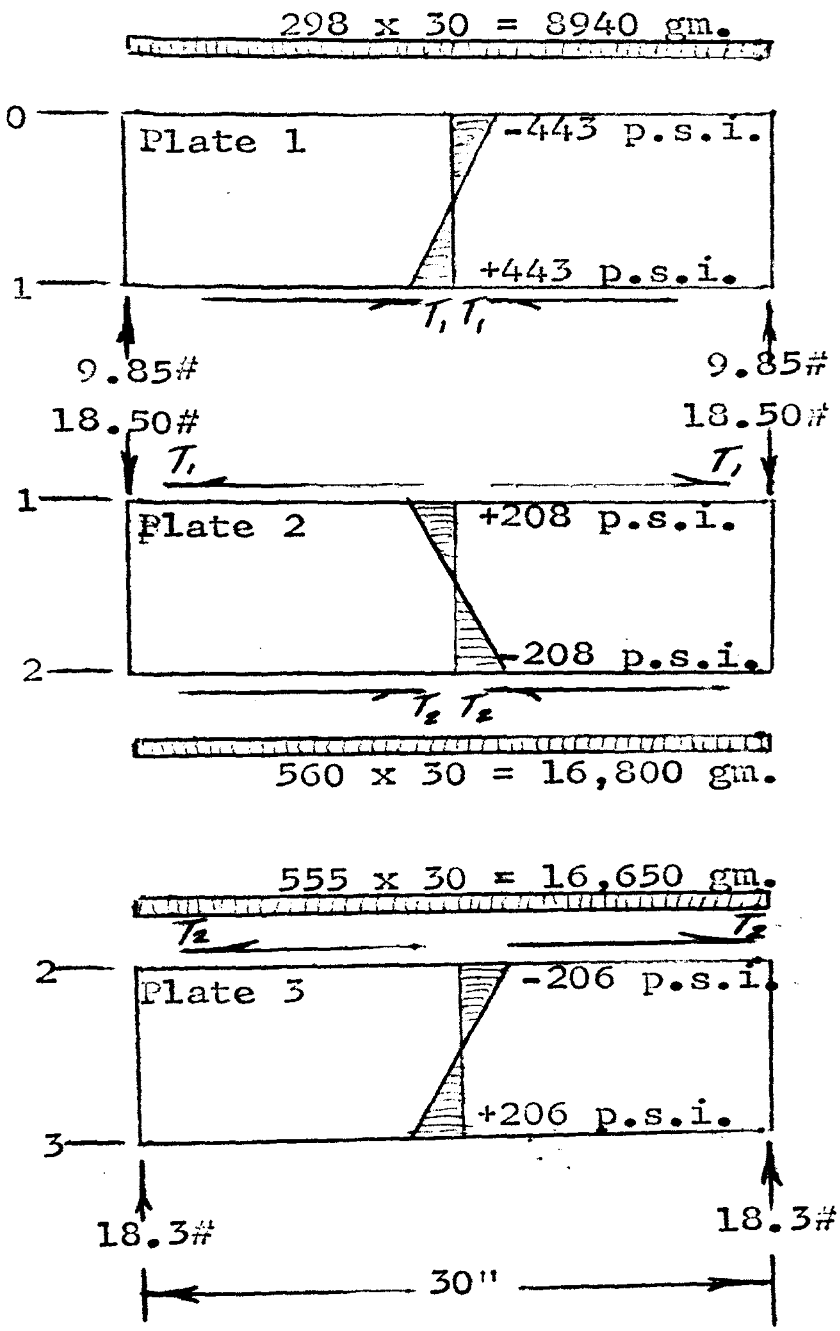

$$M_{o_1} = \frac{-(8940)(30)}{8}$$
$$= 33,500 \text{ in-gm.}$$

$$\sigma_{o_{10}} = \frac{33,500}{.167}$$
$$= 201,000 \text{ gm/in}^2.$$
$$= 443 \text{ p.s.i.}$$

Similarly, the stresses at all the ridges are found.

Solving for T_1 and T_2 : Since the shearing force is the only longitudinal force acting on the plates, the internal reactions must consist of an axial force and a moment as shown below.

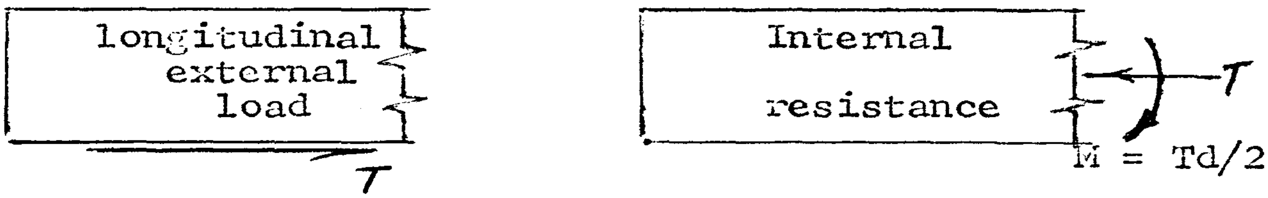

Therefore the stresses at the edges of the plates can be put in terms of the bending stresses, T_1, and T_2 .

$$\sigma_{1_0} = -443 - \frac{T_1}{.354} \quad \frac{T_1\,(2.83/2)}{.167} \quad = -443 + 5.68\ T_1$$

Similarly,

$$\begin{aligned}
\sigma_{1_1} &= +443 - 11.32\ T_1 \\
\sigma_{2_1} &= +208 + 5.66\ T_1 + 2.83\ T_2 \\
\sigma_{2_2} &= -208 - 2.83\ T_1 - 5.66\ T_2 \\
\sigma_{3_2} &= -206 + 5.66\ T_2 \\
\sigma_{3_3} &= +206 - 2.83\ T_2
\end{aligned}$$

From the boundary condition that $\sigma_{2_1} = \sigma_{1_1}$, and $\sigma_{3_2} = \sigma_{2_2}$ solving the equations simultaneously:

$$\begin{aligned}
T_1 &= 13.1\# \\
T_2 &= -3.4\#
\end{aligned}$$

Placing these back into the above equations,

$$\begin{aligned}
\sigma_{1_0} &= -369 \text{ p.s.i.} \\
\sigma_{1_1} = \sigma_{2_1} &= +295 \text{ p.s.i.} \\
\sigma_{2_2} = \sigma_{3_2} &= -225 \text{ p.s.i.} \\
\sigma_{3_3} &= +216 \text{ p.s.i.}
\end{aligned}$$

<u>Third</u> <u>Step</u>: Taking into account the deflection of the plates

Assuming a triangular distribution of shear (maximum at the end and zero at center line) along the edges of the plates, the deflection at the denterline of a plate is found by the following equation.

$$\delta_{℄} = \left(\frac{\sigma_c - \sigma_{℄}}{Eh}\right)\frac{L^2}{9.6}$$

Assumed deflections of plates:

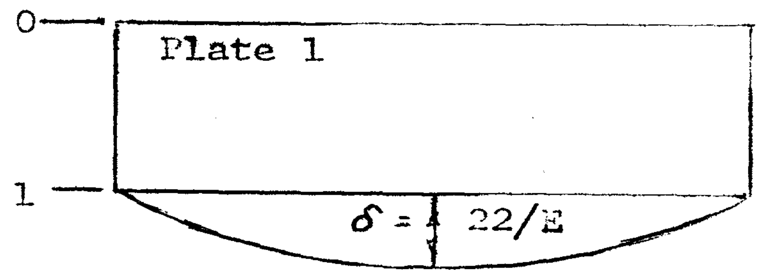

$$\delta_{\text{℄}} = \frac{(-.369-.295)\,(30)^2}{E(2.83)\quad(9.6)}$$

$$= \frac{22}{E} \text{ inches}$$

In a similar manner the deflections for plates 2 and 3 are found.

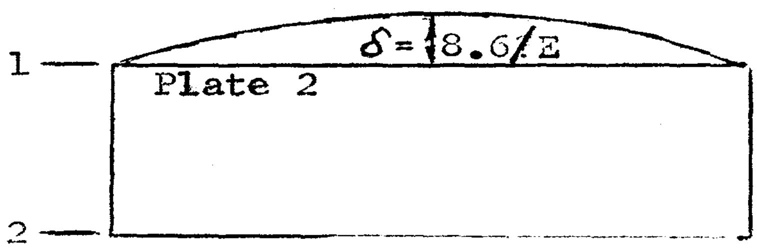

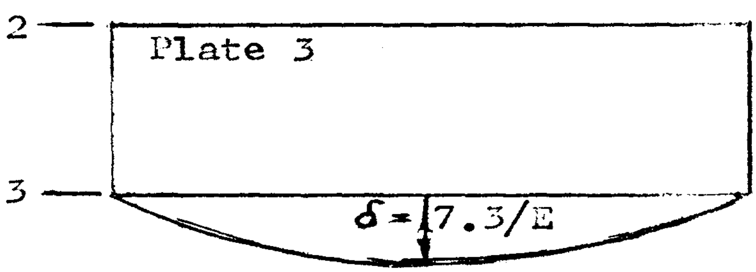

Using a graphical solution similar to a Williot diagram, the relative deflections of the ridges are obtained. Since all the ridges do not settle the same amount, they cause an additional transverse moment at each ridge that was not accounted for previously. This moment is equal to $6EI\Delta/L^2$, where Δ = the differential settlement of one ridge in respect to another. Using these moments, a moment distribution was carried out, but it was found in this case that it changed the original moments very little, so it was neglected. In most cases these cannot be neglected.

On the following page are the diagrams of plates 1 through 3 with the calculated stress for the end, quarter point and center line shown. These stresses were obtained assuming a parabolic moment distribution from zero at the ends to a maximum at the center, and a triangular shear distribution with the maximum at the end and zero at the center.

Calculated stresses in plates: (p.s.i.)

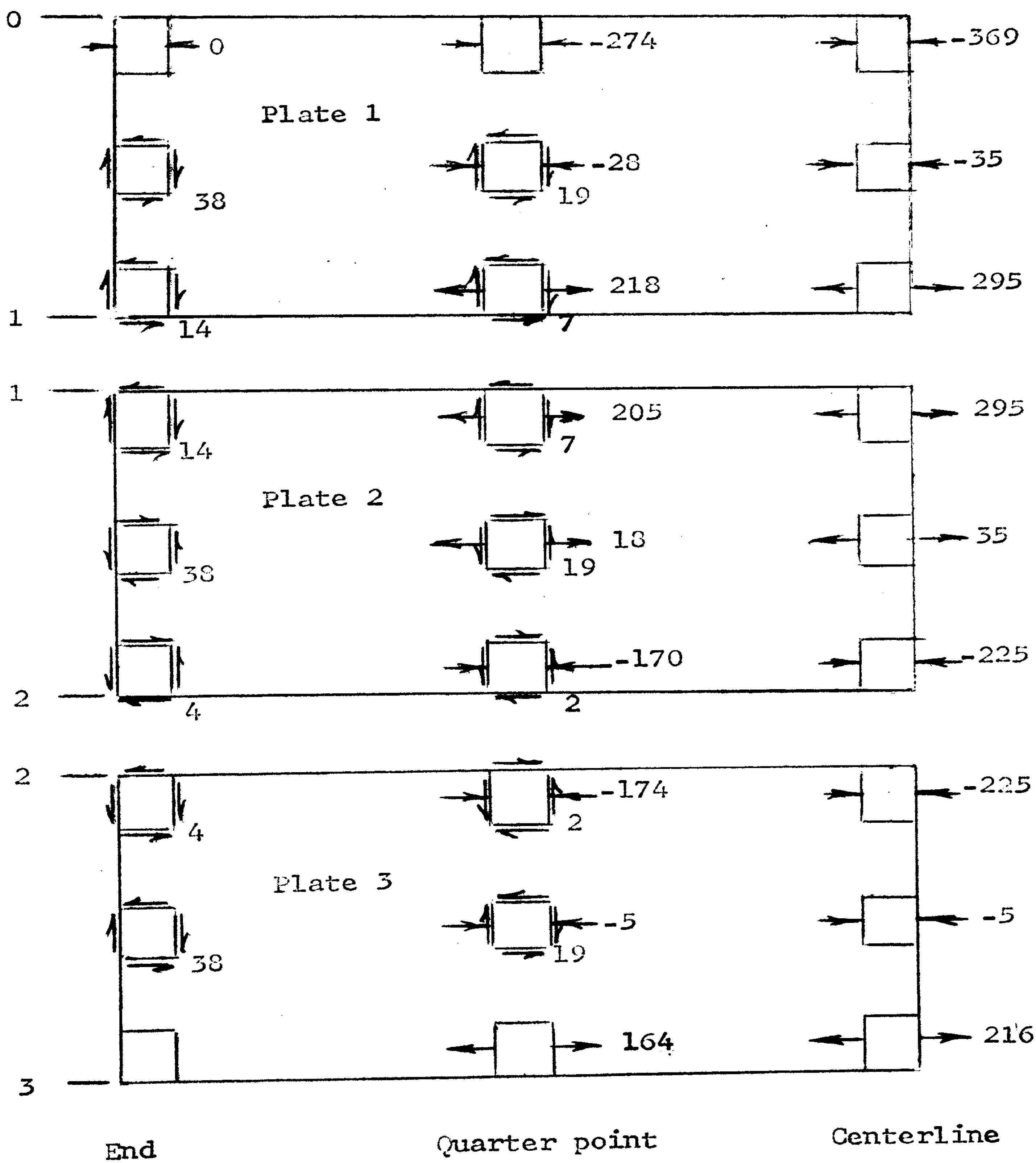

VITA

Graham G. Sutherland, III was born March 9, 1942, in Cambridge, New York, the son of G. Gardiner and Sylvia Sutherland. He received his elementary schooling in the central school system of Greenwich, New York, and attended the Burnt Hills - Balston Lake High School in Burnt Hills, New York, graduating in 1960. In the fall of 1960 he enrolled in the Missouri School of Mines and Metallurgy, Rolla, Missouri. In the spring of 1964 he received a Bachelor of Science Degree in Civil Engineering. He entered graduate school in the fall of 1964 as a National Science Foundation Cooperative Fellow and part-time instructor in the Civil Engineering Department.